MODELLING AND CONTROLS OF A HEXACOPTER

A Thesis

by

KULDEEP SINGH

Submitted to the College of Graduate Studies
Texas A&M University - Kingsville
in partial fulfillment of the requirements for the degree of

MASTER OF SCIENCE

December 2018

Major Subject: Mechanical Engineering

MODELLING AND CONTROLS OF A HEXACOPTER

A Thesis

by

KULDEEP SINGH

Approved as to style and content by:

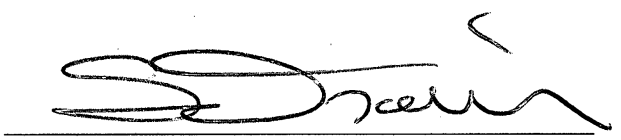

Selahattin Ozcelik, Ph.D.
(Chair of Committee)

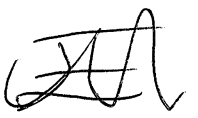

Dervis Emre Demirocak, Ph.D.
(Member of Committee)

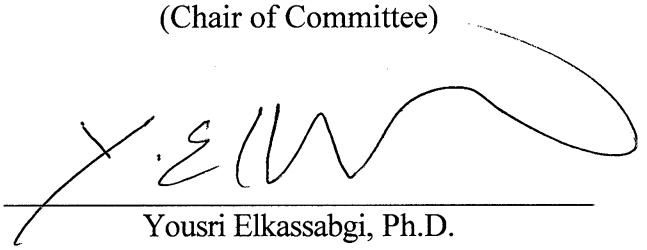

Yousri Elkassabgi, Ph.D.
(Member of Committee)

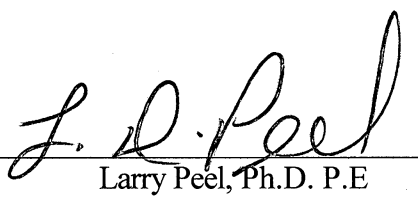

Larry Peel, Ph.D. P.E
(Chair of Department)

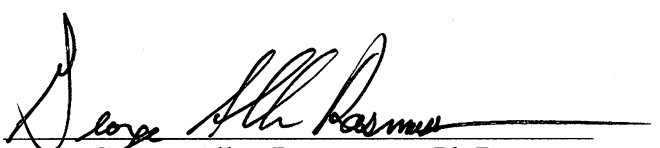

George Allen Rasmussen, Ph.D.
(Vice President for Research and Graduate Studies)

December 2018

ABSTRACT

Modelling and Controls of a Hexacopter

(December 2018)

Kuldeep Singh, B.Tech, RTU, Kota, Rajasthan, India.

Chair of Advisory Committee: Dr. Selahattin Ozcelik

Multicopters also known as drones, are becoming a common platform for the Unmanned Aerial Vehicles (UAVs). These devices are usually powered and propelled by multiple rotors placed in a geometric arrangement around the drone to allow control of the drone during flight. The main purpose of this research is to present the basic mathematical model for a Hexacopter, which is a special type of drone and to design a control scheme for the safe operation of the Hexacopter. In a hexacopter, three pairs of counter-rotating fixed blades are placed around the hexacopter. A Hexacopter is not as popular as a quadcopter but has several advantages over the quadcopter including vertical landing and takeoff, hovering, the capability of performing more complex operations over other aircraft. The hexacopter is controlled by adjusting the angular velocities of the rotors which are further controlled by a flight controller.

In this thesis, a mathematical model of a hexacopter is formulated to study the dynamic behavior of the Hexacopter. A suitable control is built for improving the hovering conditions and to control the attitude (Roll, Pitch, and Yaw) of the hexacopter. The multirotor is assumed as a rigid body, so the differential equations can be derived by Newton-Euler or the Euler-Lagrange equations. The mathematical model is designed by considering the Newton-Euler parametrization.

DEDICATION

I would like to dedicate this thesis to my father Rajendra Singh and my mother Gurmeet Kaur who have been there with me through this entire time and believed in me throughout. I would also like to dedicate this thesis to my sisters who supported and gave me the strength to reach my goal. Their constant support and belief during my entire thesis work really helped me to stay positive and keep moving forward. Without all of them, this thesis wouldn't have been possible.

ACKNOWLEDGMENTS

I would like to thank my advisor Dr. Selahattin Ozcelik whose perception, support and knowledge have guided me throughout the course of my thesis. My genuine thanks to Dr. Yousri Elkassabgi and Dr. Dervis Emre Demirocak for being my committee members and helping me with this thesis. I would like to thank the whole faculty staff of Mechanical Engineering for enlightening me with their knowledge throughout my coursework at this university. I would also like to thank Sarvesh and Akshay for their constant support and advice in completing my thesis. And finally, I would like to thank my friends Paritosh and Nikhil for their support throughout my graduate program.

TABLE OF CONTENTS

LIST OF FIGURES

Page

LIST OF TABLES

Page

CHAPTER I

INTRODUCTION

1.1 Background

The study and research on Unmanned Aerial Vehicles (UAVs) are growing rapidly. UAVs have become a common source to capture information from various fields like Military operations, Sports, Weather, Traffic, Search, and Rescue and many more. During the early stages the research was limited to four rotor copters known as the Quadcopters but now researchers have increased their vision to Hexacopters and Octocopters because they have various advantages over the Quadcopters [4], [1]. For example, Hexacopters show more flight time, they have better fault tolerance capacity compared to a Quadcopter, they can carry more load compared to a Quadcopter. Furthermore, the use of more than one motor decreases the length of the blades leading to less dynamical and structural problems. UAVs even enjoy various advantages over the land robots like they are excellent for the surveillance purpose, they can be used for search and rescue operations, drones can also be used to spray chemicals on an agricultural field, they can modulate distance from the ground and can spray in real time for an even coverage increasing the overall efficiency of the field [17]. A hexacopter is basically a 6-rotor helicopter. Its thrust or upward force is provided by the 6 rotors equally and other movements can be controlled by varying the speed of the motors. Drones can also be used for aerial photography search and rescue operations, 3D mapping, pipe inspections, for delivering packages in remote areas etc. A hexacopter has 6 rotors arranged clockwise and counter-clockwise that work together to provide the upward thrust and negates the need to counteract

---

This thesis follows the format used by IEEE Journal on Robotics and Automation.

aerodynamic torque forces. It divides the thrust needed for flight by 1/6 for each rotor thus letting the use of less powerful motors which can help in reducing costs without compromising with the overall efficiency.

Figure 1. Hexacopter with a surveillance camera [16]

A hexacopter consists of the following parts: Chassis, Motor, Propellers, Flight controller, Transmitter and Receiver, Electronic speed controller, Battery, and battery charger.

- Chassis:

The Chassis is shown in Figure (2) below. It is the base of a Hexacopter, it gives the shape and stability to the hexacopter [13]. The chassis is like the skeleton to the hexacopter. The frame should be strong and light in weight at the same time. It should be strong to carry enough load and light so that it can provide a sufficient amount of flight. It can be made of different materials based on the efficiency, stiffness, operation required to be performed, two such materials are Carbon Fiber and Aluminum.

Figure 2. Chassis of a Hexacopter [18]

- Motor:

A motor is shown below in Figure 3. A motor is one of the most important parts of a hexacopter [12], [13]. There is one motor for each propeller, the motors on each propeller should be of the same dimensions and it is calculated in kV. The more the kV the faster the motor can spin. But, the faster the motor spins the lesser is the flight time because it extracts more power from the battery.

Figure 3. The motor of a Hexacopter [14]

- Propeller:

A motor drives the propellers and they are responsible for the flight. A hexacopter has six propellers three clockwise and three counterclockwise [13]. Propellers are shown in Figure 4. Propellers are responsible for the speed of flight and capacity to take the load. Longer propellers take a longer time to speed up and slow down, but it can achieve stronger lift with low RPM. Shorter propellers give the tendency to vary speed more quickly however they require more energy to spin.

Figure 4. Propellers [13]

- Flight Controller:

The flight controller is shown in Figure 5 below. The flight controller is like the motherboard of the hexacopter [12], [13]. It directs the RPM of each motor in response to the given input. A command is fed into the flight controller by the pilot to move the multi-rotor in forwarding/backward direction, it then adjusts the motors according to the given command.

Figure 5. Flight controller for a Hexacopter [12]

- Transmitter and Receiver:

Figure 6 shows a Transmitter and Receiver. The transmitter and receiver are what send and receive the signals to the hexacopter respectively [13]. The pilot sends a signal to the hexacopter to perform a certain operation during the flight, the receiver receives the signals and the flight controller acts on it. The transmitter and receiver combination is unique for every hexacopter and cannot be altered. Different channels are present on the receiver for performing different operations like flying, direction, speed, hovering etc.

Figure 6. Transmitter and Receiver [15]

- Electronic speed controller:

An Electronic Speed Controller (ESC) is shown below in Figure 7. An ESC controls the speed of the motor by supplying the exact amount of current required by the motor [12]. Each motor has a separate ESC and the size of the ESC varies with the size of the chassis of the drone or the size of the motors. ESC comes with a battery eliminator circuit which allows the transmitter to connect to the ESC rather than directly connecting it to the battery.

Figure 7. Electronic Speed Controller [12]

- Battery and Battery Charger:

A sample battery is shown in Figure 8. The main power source of the hexacopter is the battery [13]. Typically, a Lithium Polymer (Lipo) battery is used to power the hexacopter. The battery life depends on the weight of the drone, the size of the drone, the weight, and size of the motors, it depends on the operations performed by the drone.

Figure 8. Battery [19]

1.2 Problem Statement

The control of the hexacopter is complicated due to the higher number of motors attached to it. Every motor has its own weight, which in all adds to the weight of the hexacopter and therefore it is difficult to control the hexacopter and to achieve stability, hovering, and attitude (Roll, Pitch, and Yaw) of the hexacopter. Due to heavy payload the battery life decreases, overall flight time is affected which makes it a difficult problem for control system design. The mathematical modeling of the hexacopter is more complex as it involves complex equations which makes it a difficult problem to solve.

1.3 Research Objectives

a) To study the dynamics and kinematics of the hexacopter and develop an appropriate non-linear mathematical model. This model will be used to control the altitude and attitude of the hexacopter.

b) A suitable controller will be built for controlling the altitude and for controlling the attitude (Roll, Pitch, and Yaw) of the hexacopter.

c) External atmospheric factors will be introduced to the controller and their graphs will be plotted and the results will be studied.

All the above mentioned objectives were achieved.

CHAPTER II

LITERATURE REVIEW

In recent years, the research on drones has increased rapidly. Drones are a category of robots which can fly in the air to perform various tasks. Drones include Unmanned Aerial Vehicles (UAVs) and small drones that can only fly in certain confined spaces [11]. Drones have become the most popular option for various operations, basic and complex. Cheaper and more feasible drones are being built by companies, which can provide necessary assistance in industries and other fields like surveillance, military operations, agriculture, geological mapping [2], for performing inspections, they can also be used for picking and placing objects in industries, for delivering packages etc. The classification of drones can be done based on their size, based on their characteristics, based on the operations they can perform. Based on the operation the drones are classified as MAVs (micro or miniature air vehicles), NAVs (nano air vehicles), VTOL (vertical takeoff and landing), LASE (low altitude short endurance), HASE (high altitude short endurance). The basic requirements for increasing the efficiency of a drone are having the correct motor, a suitable electronic stability controller, and propellers of suitable size [15]. A hexacopter has six rotors and corresponding propellers which are 60 degrees apart from each other to provide safety control and flight to the hexacopter. In case of a motor failure, remaining motors bear the additional load of that motor so that the overall efficiency and flight time are not affected, but we have to compromise with the overall weight and increased price.

In 2013 V. Artale [1] presented a paper for the modeling of a hexacopter. The paper described the hexacopter in detail and why multi-copters with more than four rotors are coming in trend. A mathematical model was designed by using the Newton- Euler and Euler- Lagrange equations and using quaternions to avoid singularities. Quaternions were used considering the

linearity of quaternion formulation stability and efficiency.

Jeroen A.J. Ligthart presented a paper [2] for modeling and controls of a hexacopter. Mathematical modeling was done, and a controller was designed using the Model Predictive Controller (MPC). A three termed MPC cost function was used to experiment the drone indoor and outdoor to find different results. However, the experimental validation and theoretical analysis were not completed.

Moussid [3] presented a paper which showed detailed modeling of the Hexarotor using the Newton-Euler method. A linear and a non-linear controller were built using the PID controller design and the Backstepping and Sliding Mode (SMC) design and the results were compared, and the non-linear controller was found giving average results.

Andrea Alaimo [4] in 2013 presented a paper in which a mathematical model and a linear PID controller were designed for a hexacopter and results were tested. The Newton-Euler method was used to design the model for the hexacopter. Quaternions were used to improve the stability and efficiency of the controller algorithm. The model and algorithm were tested, and the model was validated using various experiments in which the drone was kept moving to note the elementary trajectories.

Diana Ovalle [5] presented a paper in which a mathematical model was designed using force and torque as control variables. Finally, a nonlinear optimal control problem was formulated to see the hexacopter maneuverability capabilities which clearly showed the difficulties in moving x and y coordinate directions due to lack of actuators on those axes.

Guillermo P. Falconi [6] presented a paper in which a position control was designed for a hexacopter. An extra controller was used whose purpose was to reject the modeling error. The most common approach is to use the Failure Detection and Isolation (FDI) filter and then

reconfigure the controller but the FDI is very complex for the hexacopter so Modified Linear Extended State Observer (LESO) was used with the controller which does not adopt the strategy of failure detection or reconfiguration. The controller achieved a safe flight but still, more work needs to be done for improving the performance during the flight.

O. A. Ahmed [7] presented a paper in February 2015 based on the modeling and the visual serving controller for a hexacopter in which pitching torque was used based on desired pitching angle to get the translation motion which could move the hexacopter in the forward and backward direction. Further, the lateral motion was achieved by using desired rolling torque based on rolling angle which could move the hexacopter in left or right direction. The altitude and heading were achieved by using a PD controller with multiple gains to control the speed of the hexacopter.

Radek Baranek and his team proposed a paper [8] in which the basic modeling and controls of a hexacopter were presented, the model was designed using the proposed control law. The control law was partially implemented RC (Radio controlled) micro-copter, it required fast response from the actuators and fast processing of control algorithms.

Robert Leishman in 2012 presented a paper [9] in which a multi-copter was developed with vision-based ability to work in a GPS-denied environment. EKF was used by the team for localization and mapping. EKF stands for Extended Kalman Filter which uses maximum likelihood algorithm for data association, the navigation controller based on EKF is strong and provides quality of information. Future work still needs to be done which includes designing of the appropriate algorithm for the design presented.

Models of UAVs like, Perley's plane, were used as flying explosives attached with timing hardware which were expected to drop in enemy areas. After the first Gulf War, advancement in

UAV innovation increased at a tremendous rate in the United States. While a major portion of the funding has been used for aviation and military purposes, commercial and hobby-grade UAV usage has also increased. Instead of contributing a huge amount to regular helicopters and pilots the media is also using UAVs for filming live incidents whether it be for weather forecasting or covering road accidents and many more.

Designing of UAVs or Unmanned Aerial Combat Vehicles (UACVs) is less complicated as it is just driven by aerodynamics and its payload. The UCAVs are transforming wars by replacing manned flights and helping to maintain a safe amount of distance from the war field. There were only around fifty UAVs in the most recent decade, but at this point, the Department of Defense has around seven thousand UAVs and Micro Aerial Vehicles (MAVs) [20].

The Australian National University [21] designed a controller to stabilize the dominant decoupled pitch and roll modes and use a model of disturbance inputs to estimate the overall performance of the system and it was found that the compensator successfully regulated the attitude at even lower rotor speeds. The flyer attitude dynamics was analyzed which allowed tuning the mechanical design of the quad-rotor for best control sensitivity and disturbance rejection.

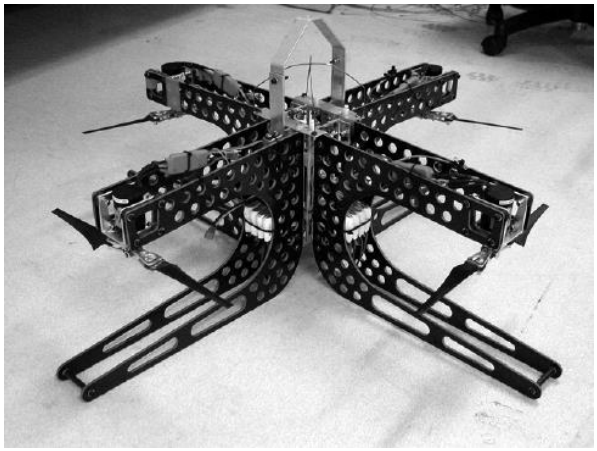

Figure 9. X-4 Flyer Mark II [21]

Holger Voos [22] presented a work to develop an inner and an outer loop attitude-controlled quadrotor UAV. The dynamic model of the quadrotor was derived using MATLAB/SIMULINK simulation model. With the help of that simulation, the non-linear vehicle control system was tested, and its efficiency was demonstrated.

S. Bouabdallah and R. Siegwart [23] created a small UAV called OS4 and used a model-based controller to demonstrate the automatic take-off, hover, avoid collisions and landing of the UAV. Real experiments were conducted with the same control parameters tuned in the simulation which permitted the design of the controller for the take-off, hover, avoid collisions and landing of the UAV.

Akshay Pawar, S. G. Joshi, and V.P. Sulakhe [24] presented a paper. The design and development of an autopilot system for a UAV Hexacopter were done using onboard computing, then the hovering for the UAV was successfully tested. A successful demonstration was done for the stabilization of the UAV's heading, pitch, altitude, and roll consuming lesser power and increasing the overall payload.

Atheer L. Salih [25] along presented the design of an algorithm used to control the quadcopter system. A four-rotor vertical take-off and landing (VTOL) UAV known as quad-rotor aircraft was modeled then the model was modified to simplify the controller and convert the resulting mathematical model to the respective Simulink model for ease of simulation and further study of the quad-rotor system.

Pakom Poksawat and Liuping Wang [26] presented a novel approach to automatic tuning of the PID controller for a Hexacopter. A relay feedback control for the hexacopter was conducted in a controlled environment for operational safety through an experimental setup. The relay experimental testing data were used to design the suitable PID controller and to identify the dynamics of the hexacopter.

Dang Khanh and Taek-Kun Nam [27] presented a paper on a study on the modeling of a hexacopter in which a mathematical model of a hexacopter was presented. The equations of motion were defined by using quaternions since the quaternions do not suffer gimbal lock, all the equations of motion for moment and force were defined in detail. The Newton-Euler method was taken into consideration to design the model of the hexacopter. Both PD and PID controllers were implemented to build the controller and the simulation results were analyzed and presented in the paper.

Simanti Bose, Adrija Bagchi, and Naisargi Dave [28] presented a paper in which MPU Sensor was used to sense the real-time position of the hexacopter which helped in getting more stable values of the control inputs. PID tuning was used to control the control inputs which allowed the fine tuning of the inputs for the desired controller.

CHAPTER III

SYSTEM MODELING

This section will deal with the methods used to build the mathematical model for the hexacopter. It deals with the coordinate frames chosen and the reference frame chosen to describe the dynamics of the hexacopter. The angular orientation of the aircraft is described by the three angles (Roll, Pitch, and Yaw) that govern the flight of the hexacopter, these are called the Euler Angles. These Euler angles represent an ordered set of sequential equations between the reference frame and the body frame.

3.1 Euler Angles

Leonhard Euler described the Euler angles [10]. These angles describe the angular orientation of a fixed body with respect to a reference frame. The Euler angles for the aircraft are Yaw (ψ), Pitch (θ), and Roll (ϕ). Yaw angle originates due to the center of gravity and is perpendicular to the wings. Pitch angle originates due to the center of gravity and goes parallel to the wingtip. Roll angle originates due to the center of gravity and goes parallel to the wings of the aircraft.

The schematic of the hexacopter is presented below [1]. Two frames describe the motion of the hexacopter which are Inertial or Fixed frame and the Body frame. The motion of an aircraft is planned by geographical coordinates, so it is useful to define an earth-fixed frame tangent to the earth surface. The Euler angles Yaw (ψ), Pitch (θ), and Roll (ϕ) define the angular position of the Body frame with respect to the Inertial frame.

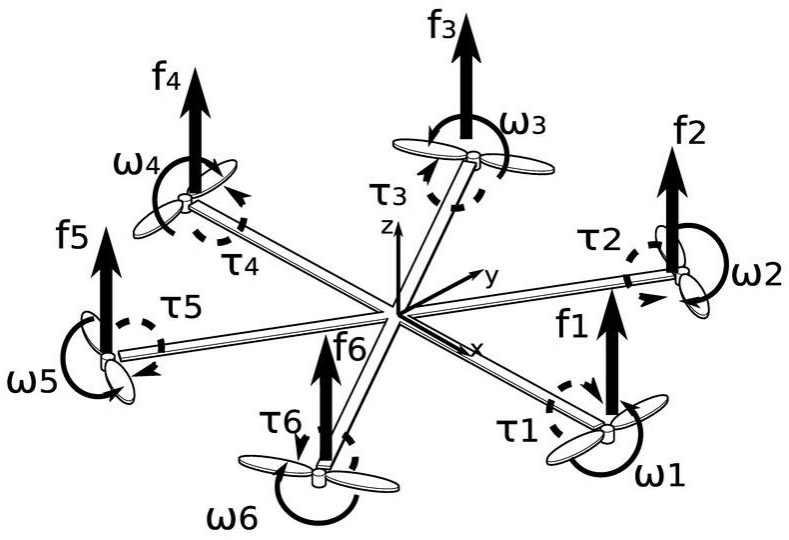

Figure 10. Schematic of a Hexacopter [1]

For making it simpler let us take linear position vector and rotational position (Euler angle) vector in the inertial frame by means of $X = [\ x\ y\ z]^T$ and $\eta = [\phi\ \theta\ \psi]^T$, respectively. Therefore, the linear velocities and angular velocities in the inertial frame will be $\dot{X} = [\dot{x}\ \dot{y}\ \dot{z}]^T$ and $\dot{\eta} = [\dot{\phi}\ \dot{\theta}\ \dot{\psi}]^T$ [1]. Now, we define the transformation from the body frame to the inertial frame using the rotation matrix **R** which is orthogonal. **R** can be defined by the combined rotation along x, y, and z-axis:

Rotation along the x-axis can be written as:

$$R_x = \begin{bmatrix} 1 & 0 & 0 \\ 0 & cos\phi & -sin\phi \\ 0 & sin\phi & cos\phi \end{bmatrix} \quad (1)$$

Rotation along y-axis can be written as:

$$R_y = \begin{bmatrix} cos\theta & 0 & sin\theta \\ 0 & 1 & 0 \\ -sin\theta & 0 & cos\theta \end{bmatrix} \quad (2)$$

Rotation along the z-axis can be written as:

$$R_z = \begin{bmatrix} cos\psi & -sin\psi & 0 \\ sin\psi & cos\psi & 0 \\ 0 & 0 & 1 \end{bmatrix} \quad (3)$$

Rotation matrix R = $R_x * R_y * R_z$

$$\mathbf{R} = \begin{bmatrix} cos\theta cos\psi & cos\psi sin\theta sin\phi - cos\phi sin\psi & cos\phi cos\psi sin\theta + sin\phi sin\psi \\ cos\theta sin\psi & cos\phi cos\psi + sin\theta sin\phi sin\psi & cos\phi sin\theta sin\psi - cos\psi sin\phi \\ -sin\theta & cos\theta sin\phi & cos\theta cos\phi \end{bmatrix} \quad (4)$$

The transformation matrix from the inertial frame to the body frame will be $\mathbf{R^{-1}} = \mathbf{R^T}$ respectively.

In order to achieve continuity in the system while transforming from the body frame to inertial frame, we have to obtain transformation matrix for angular velocities [1]. The z-y-x sequence of rotation is followed i.e. first rotation about $\dot{\boldsymbol{\psi}}$ takes place which has to cover two rotations R_x and R_y in order to reach body frame, then rotation about $\dot{\boldsymbol{\theta}}$ takes place which has to undergo rotation about R_x in order to align with the body frame and finally rotation about $\dot{\boldsymbol{\phi}}$ takes place which does not has to undergo any rotations.

The transformation laws are $\nu = \omega_\eta \dot{\eta}$ and $\dot{\eta} = \omega_\eta^{-1} \nu$ in which the angular velocity ν is defined by the vector $\nu = [p \quad q \quad r]^T$. $\mathbf{W}_\eta^{-1}$ can only be defined if $\theta \neq \pi/2 + k\pi$ where k =$(k \in Z)$.

$$\begin{bmatrix} p \\ q \\ r \end{bmatrix} = \begin{bmatrix} \dot{\phi} \\ 0 \\ 0 \end{bmatrix} + Rx \begin{bmatrix} 0 \\ \dot{\theta} \\ 0 \end{bmatrix} + RxRy \begin{bmatrix} 0 \\ 0 \\ \dot{\psi} \end{bmatrix} \quad (5)$$

$$\begin{bmatrix} p \\ q \\ r \end{bmatrix} = \begin{bmatrix} \dot{\phi} \\ 0 \\ 0 \end{bmatrix} + \begin{bmatrix} 1 & 0 & 0 \\ 0 & cos\phi & -sin\phi \\ 0 & sin\phi & cos\phi \end{bmatrix} \begin{bmatrix} 0 \\ \dot{\theta} \\ 0 \end{bmatrix} + \begin{bmatrix} 1 & 0 & 0 \\ 0 & cos\phi & -sin\phi \\ 0 & sin\phi & cos\phi \end{bmatrix} \begin{bmatrix} cos\theta & 0 & sin\theta \\ 0 & 1 & 0 \\ -sin\theta & 0 & cos\theta \end{bmatrix} \begin{bmatrix} 0 \\ 0 \\ \dot{\psi} \end{bmatrix} \quad (6)$$

$$\begin{bmatrix} p \\ q \\ r \end{bmatrix} = \begin{bmatrix} 1 & 0 & -sin\theta \\ 0 & cos\phi & cos\theta sin\phi \\ 0 & -sin\phi & cos\theta cos\phi \end{bmatrix} \begin{bmatrix} \dot{\phi} \\ \dot{\theta} \\ \dot{\psi} \end{bmatrix} \quad (7)$$

Where the transformation matrix for angular velocities from the inertial frame to body frame is:

$$\omega_{\eta} = \begin{bmatrix} 1 & 0 & -sin\theta \\ 0 & cos\phi & cos\theta sin\phi \\ 0 & -sin\phi & cos\phi cos\theta \end{bmatrix} \tag{8}$$

The transformation matrix for angular velocities from body frame to inertial frame will be:

$$\omega_{\eta}^{-1} = \begin{bmatrix} 1 & sin\phi tan\theta & cos\phi tan\theta \\ 0 & cos\phi & -sin\phi \\ 0 & sec\theta sin\phi & cos\phi sec\theta \end{bmatrix} \tag{9}$$

The total rotational rate vector is:

$$\omega = \dot{\phi} + \dot{\theta} + \dot{\psi} \tag{10}$$

Therefore, angular velocity vector will be $\omega = \nu = \boldsymbol{\omega}_{\eta}\dot{\eta}$

$$\nu = \begin{bmatrix} p \\ q \\ r \end{bmatrix} = \begin{bmatrix} 1 & 0 & -sin\theta \\ 0 & cos\phi & cos\theta sin\phi \\ 0 & -sin\phi & cos\phi cos\theta \end{bmatrix} \begin{bmatrix} \dot{\phi} \\ \dot{\theta} \\ \dot{\psi} \end{bmatrix} \tag{11}$$

Now, we will represent the hexacopter as a solid body in 3-D space. The flexibility of the blades as well as the six electric motor dynamics will be neglected as the motor dynamics is relatively fast. The motion of a rigid body can be broken down into translation and rotational components. To describe the dynamics of the hexacopter Newton-Euler equations that govern linear and angular motion are considered.

Inertial Matrix: The hexacopter is assumed to have a symmetric structure with the six arms aligned with the body x & y-axis [1].

$$I = \begin{bmatrix} I_{xx} & 0 & 0 \\ 0 & I_{yy} & 0 \\ 0 & 0 & I_{zz} \end{bmatrix} \tag{12}$$

3.2 Newton-Euler equations

Newton-Euler equations describe the complete dynamics (Rotational and Translational) of a rigid body. The Newton-Euler equations combine two equations Newton's equations and Euler equations into a single equation with six components using matrices and column vectors [10]. These equations relate the center of gravity with the sum of torques and forces acting on the body. According to the Newton-Euler equations, the sum of the angular acceleration of the inertial frame, the centripetal force, and the gyroscopic force is equal to the external torque of the hexacopter. With reference to the coordinate frame whose origin coincides with the center of mass of the body, the Newton-Euler equations can be represented as:

$$m\dot{V}_B + \nu \times (mV_B) = \mathrm{F} \tag{13}$$

$$\mathrm{F} = \mathrm{F_g} + \mathrm{T_B}$$

where,

F= total force acting on the center of mass

m= mass of the body

F_g = gravitational force

T_B = total thrust

$\nu \times (mV_B)$ = centrifugal force

- **Translational dynamics**:

Thrust force generated by motor 1 is given by:

$$\mathrm{T_{hi}} = k\omega^2 \tag{14}$$

Where,

k = lift constant

ω = angular velocity of the motor

T_{hi} = Thrust generated by each propeller

Now, since there are 6 motors and every motor generates a thrust, the total thrust will be:

$$T_B = \sum_{i=1}^{6} T_{hi} \tag{15}$$

$$= k\begin{bmatrix} 0 \\ 0 \\ \sum \omega_i^2 \end{bmatrix}$$

$$= k\begin{bmatrix} 0 \\ 0 \\ \omega_1^2 + \omega_2^2 + \omega_3^2 + \omega_4^2 + \omega_5^2 + \omega_6^2 \end{bmatrix}$$

The total thrust will be:

$$F = F_g + T_B \tag{16}$$

F_g = Gravitational force

T_B = Total thrust

Total Thrust:

$$T_B = k\begin{bmatrix} 0 \\ 0 \\ \omega_1^2 + \omega_2^2 + \omega_3^2 + \omega_4^2 + \omega_5^2 + \omega_6^2 \end{bmatrix} \tag{17}$$

The linear motion in the body frame can be summarized as:

$$m\ddot{X} = \begin{bmatrix} 0 \\ 0 \\ -mg \end{bmatrix} + T_B \tag{18}$$

Taking m on the other side:

$$\begin{bmatrix} \ddot{x} \\ \ddot{y} \\ \ddot{z} \end{bmatrix} = \begin{bmatrix} 0 \\ 0 \\ -g \end{bmatrix} + \frac{TB}{m} \tag{19}$$

Now if we convert the body frame to inertial frame and integrate twice we can get the position:

$$\begin{bmatrix} \ddot{x} \\ \ddot{y} \\ \ddot{z} \end{bmatrix} = \begin{bmatrix} 0 \\ 0 \\ -g \end{bmatrix} + \frac{RTB}{m} \tag{20}$$

On integrating twice, we get $[\ x\ y\ z]^T$.

Solving for $\frac{RTB}{m}$:

$$\frac{TB}{m} = \frac{k}{m}\begin{bmatrix} 0 \\ 0 \\ \omega_1^2 + \omega_2^2 + \omega_3^2 + \omega_4^2 + \omega_5^2 + \omega_6^2 \end{bmatrix} \tag{20.1}$$

$$\frac{RTB}{m} = \frac{k}{m}\begin{bmatrix} 0 \\ 0 \\ \omega_1^2 + \omega_2^2 + \omega_3^2 + \omega_4^2 + \omega_5^2 + \omega_6^2 \end{bmatrix}\begin{bmatrix} \cos\psi\sin\theta\cos\phi + \sin\psi\sin\phi \\ \sin\psi\sin\theta\cos\phi - \cos\psi\sin\phi \\ \cos\theta\cos\phi \end{bmatrix} \tag{20.2}$$

$$\ddot{x} = \frac{k}{m}\begin{bmatrix} 0 \\ 0 \\ \omega_1^2 + \omega_2^2 + \omega_3^2 + \omega_4^2 + \omega_5^2 + \omega_6^2 \end{bmatrix}[\cos\psi\sin\theta\cos\phi + \sin\psi\sin\phi] \tag{21}$$

$$\ddot{y} = \frac{k}{m}\begin{bmatrix} 0 \\ 0 \\ \omega_1^2 + \omega_2^2 + \omega_3^2 + \omega_4^2 + \omega_5^2 + \omega_6^2 \end{bmatrix}[\sin\psi\sin\theta\cos\phi - \cos\psi\sin\phi] \tag{22}$$

$$\ddot{z} = \frac{k}{m}\begin{bmatrix} 0 \\ 0 \\ \omega_1^2 + \omega_2^2 + \omega_3^2 + \omega_4^2 + \omega_5^2 + \omega_6^2 \end{bmatrix}[\cos\theta\cos\phi] - g \tag{23}$$

Integrating twice the values of $(\ddot{x}, \ddot{y}, \ddot{z})^T$ $(x, y, z)^T$.

Calculating the Torques:

The drag equation from fluid dynamics gives us the frictional force:

$$F_D = \frac{1}{2}\rho C_D A\, v^2 \tag{24}$$

ρ = Density

A = propeller area

C_D = dimensionless constant

v^2 = velocity of the propeller

hence torque on the tip of the propeller due to drag force:

$$\tau_D = \frac{1}{2}\, R\rho C_D A\, v^2 \tag{25}$$

R = Radius of the propeller

$v^2 = \omega R^2$

or,

$$\tau_D = \frac{1}{2}\, R\rho C_D A\, v^2 = b\omega^2 \tag{26}$$

b = Appropriately Dimensioned constant

The complete torque about z-axis for a motor will be:

$$\tau_{zi} = b\omega_i^2 + I_{Mi}\omega_i \tag{27}$$

I_{Mi} = Inertia moment of the i^{th} motor

ω_i = Angular velocity for the i^{th} motor

from the geometrical structure of the hexacopter and from components of T_B and τ_{zi} we can get information on the roll, pitch, and yaw.

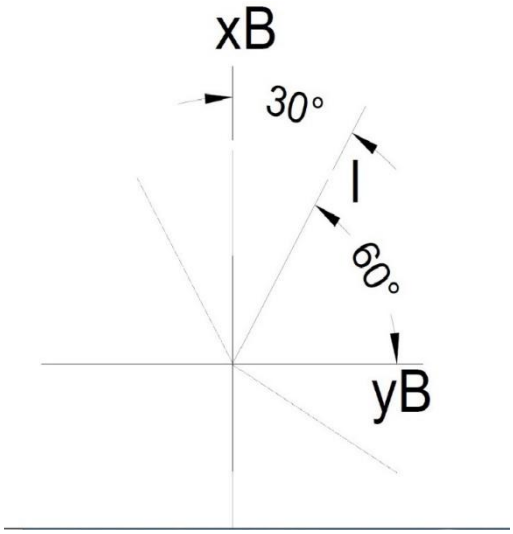

Figure 11. The geometry of the Hexacopter

Roll: In rolling motion only angular velocities ω_2, ω_3, ω_5, ω_6 are active with ω_2 and ω_3 acting in one direction and ω_5 and ω_6 acting in opposite direction. Rolling movement can be achieved by increasing or decreasing the speed of rotors on the right side and decreasing or increasing the speed of rotors on the left side at the same speed. Rolling motion is described in Figure 12 below. Here, the black arrow means the angular velocity is not changing, the red arrow means the angular velocity is decreasing, and the green arrow means the angular velocity is increasing.

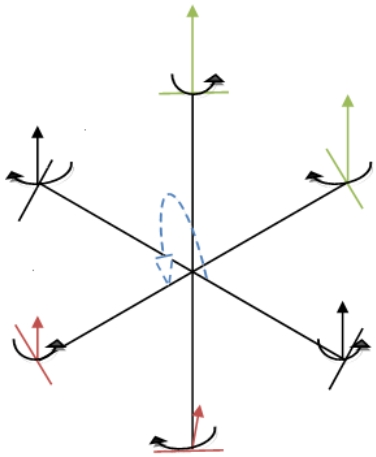

Figure 12. Rolling motion

i = 2, 3, 5, 6

consider ‘l’ as the distance of arm:

$$\tau_{\phi} = \sum l * T_B = \sin 60^{\circ} kl(\omega_2^2 + \omega_3^2 - \omega_5^2 - \omega_6^2) \quad (28)$$

Pitch: For pitch motion, angular velocities ω_1, ω_2, and ω_6 will act in one direction while ω_3, ω_4, and ω_5 will act in opposite direction. Pitching movement can be achieved by increasing or decreasing the speed of rear rotors and decreasing or increasing the speed of front rotors at the same speed. Pitch motion is described in Figure 13 below.

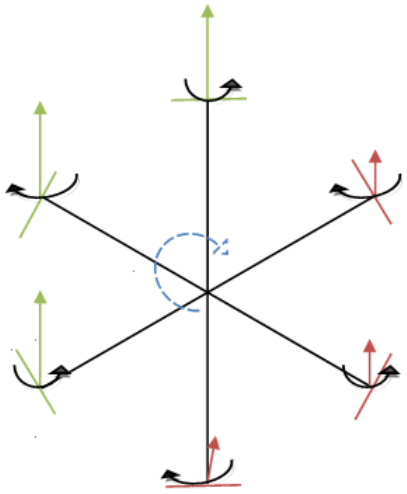

Figure 13. Pitching motion

I = 1, 2, 3, 4, 5, 6

$$\tau_{\theta} = \sum l * T_B = kl(-\omega_1^2 - \omega_2^2/4 + \omega_3^2/4 + \omega_4^2 + \omega_5^2/4 - \omega_6^2/4) \quad (29)$$

Yaw: The total torque in the z-direction can be obtained by increasing or decreasing the speed of rotors rotating clockwise while decreasing or increasing the speed of rotors rotating counter-clockwise i.e. angular velocities ω_1, ω_3 and ω_5 will act in one direction whereas angular

velocities ω_2, ω_4 and ω_6 will act in opposite directions. The yawing motion is described in Figure 14 below.

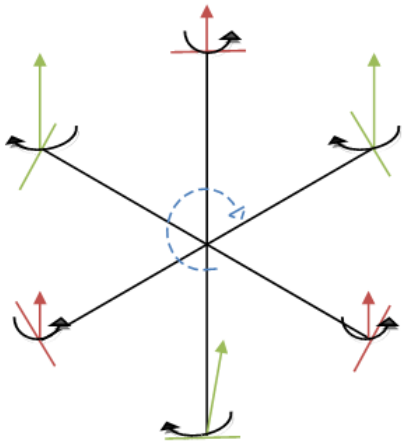

Figure 14. Yawing motion

$$T_\psi = b(-\omega_1^2 + \omega_2^2 - \omega_3^2 + \omega_4^2 - \omega_5^2 + \omega_6^2) \quad (30)$$

therefore, the total torque on the body can be represented as:

$$\tau_B = \begin{bmatrix} \tau\phi \\ \tau\theta \\ \tau\psi \end{bmatrix} = \begin{bmatrix} \frac{3}{4}kl(\omega_2^2 + \omega_3^2 - \omega_5^2 - \omega_6^2 \\ kl(-\omega_1^2 - \frac{\omega_2^2}{4} + \frac{\omega_3^2}{4} + \omega_4^2 + \frac{\omega_5^2}{4} - \frac{\omega_6^2}{4} \\ b(-\omega_1^2 + \omega_2^2 - \omega_3^2 + \omega_4^2 - \omega_5^2 + \omega_6^2) \end{bmatrix} \quad (31)$$

- **Rotational dynamics**:

Rotational dynamics equation can be governed by:

$$I\dot{\nu} + \nu \times (I\nu) + \Gamma = \tau_B \quad (32)$$

Where,

ν = Angular velocity vector

$\dot{\nu}$ = Angular acceleration

I = Moment of Inertia vector

Γ represents the gyroscopic forces

τ_B is the external torque

$$\dot{\nu} = I^{-1}\left(\begin{bmatrix} p \\ q \\ r \end{bmatrix} \times \begin{bmatrix} I_{xx} & 0 & 0 \\ 0 & I_{yy} & 0 \\ 0 & 0 & I_{zz} \end{bmatrix} \begin{bmatrix} p \\ q \\ r \end{bmatrix} - I_r \begin{bmatrix} p \\ q \\ r \end{bmatrix} \times \begin{bmatrix} 0 \\ 0 \\ 1 \end{bmatrix} \omega\Gamma + \begin{bmatrix} \tau\phi \\ \tau\theta \\ \tau\psi \end{bmatrix}\right) \tag{33}$$

$$\dot{\nu} = \begin{bmatrix} {}^{1}/_{I_{xx}} & 0 & 0 \\ 0 & {}^{1}/_{I_{yy}} & 0 \\ 0 & 0 & {}^{1}/_{I_{zz}} \end{bmatrix} \left(\begin{bmatrix} p \\ q \\ r \end{bmatrix} \times \begin{bmatrix} I_{xx}.p \\ I_{yy}.q \\ I_{zz}.r \end{bmatrix} - I_r \begin{bmatrix} p \\ q \\ r \end{bmatrix} \times \begin{bmatrix} 0 \\ 0 \\ 1 \end{bmatrix} \omega\Gamma + \begin{bmatrix} \tau\phi \\ \tau\theta \\ \tau\psi \end{bmatrix}\right) \tag{34}$$

$$\dot{\nu} = \begin{bmatrix} \frac{(I_{yy}-I_{zz})qr}{I_{xx}} \\ \frac{(I_{zz}-I_{xx})pr}{I_{yy}} \\ \frac{(I_{xx}-I_{yy})pq}{I_{zz}} \end{bmatrix} - I_r \begin{bmatrix} q(I_{xx}) \\ -p(I_{yy}) \\ 0 \end{bmatrix} \omega\Gamma + \begin{bmatrix} \tau\phi/I_{xx} \\ \tau\theta/I_{yy} \\ \tau\varphi/I_{zz} \end{bmatrix} \tag{35}$$

where,

$\omega\Gamma = -\omega_1 + \omega_2 - \omega_3 + \omega_4 - \omega_5 + \omega_6$

$$\begin{bmatrix} \dot{p} \\ \dot{q} \\ \dot{r} \end{bmatrix} = \begin{bmatrix} \frac{(I_{yy}-I_{zz})qr}{I_{xx}} \\ \frac{(I_{zz}-I_{xx})pr}{I_{yy}} \\ \frac{(I_{xx}-I_{yy})pq}{I_{zz}} \end{bmatrix} - I_r \begin{bmatrix} q(I_{xx}) \\ -p(I_{yy}) \\ 0 \end{bmatrix} \omega\Gamma + \begin{bmatrix} \tau\phi/I_{xx} \\ \tau\theta/I_{yy} \\ \tau\varphi/I_{zz} \end{bmatrix}$$

$$\dot{p} = \frac{I_{yy}-I_{zz}}{I_{xx}} qr + \frac{I_r}{I_{xx}} q\omega\Gamma + \frac{\tau\phi}{I_{xx}} \tag{36}$$

$$\dot{q} = \frac{I_{zz}-I_{xx}}{I_{yy}} qr - \frac{I_r}{I_{yy}} p\omega\Gamma + \frac{\tau\theta}{I_{yy}} \tag{37}$$

$$\dot{r} = \frac{I_{xx}-I_{yy}}{I_{zz}} pq + \frac{\tau\psi}{I_{zz}} \tag{38}$$

Integrating once will give us $(p, q, r)^T$.

Writing all the equations of acceleration,

$$\ddot{x} = \frac{k}{m}\begin{bmatrix} 0 \\ 0 \\ \omega_1^2 + \omega_2^2 + \omega_3^2 + \omega_4^2 + \omega_5^2 + \omega_6^2 \end{bmatrix} [\cos\psi\sin\theta\cos\phi + \sin\psi\sin\phi] \quad (39)$$

$$\ddot{y} = \frac{k}{m}\begin{bmatrix} 0 \\ 0 \\ \omega_1^2 + \omega_2^2 + \omega_3^2 + \omega_4^2 + \omega_5^2 + \omega_6^2 \end{bmatrix} [\sin\psi\sin\theta\cos\phi - \cos\psi\sin\phi] \quad (40)$$

$$\ddot{z} = \frac{k}{m}\begin{bmatrix} 0 \\ 0 \\ \omega_1^2 + \omega_2^2 + \omega_3^2 + \omega_4^2 + \omega_5^2 + \omega_6^2 \end{bmatrix} [\cos\theta\cos\phi] - g \quad (41)$$

$$\dot{p} = \frac{I_{yy} - I_{zz}}{I_{xx}} qr + \frac{I_r}{I_{xx}} q\omega\Gamma + \frac{\tau\phi}{I_{xx}} \quad (42)$$

$$\dot{q} = \frac{I_{zz} - I_{xx}}{I_{yy}} qr - \frac{I_r}{I_{yy}} p\omega\Gamma + \frac{\tau\theta}{I_{yy}} \quad (43)$$

$$\dot{r} = \frac{I_{xx} - I_{yy}}{I_{zz}} pq + \frac{\tau\psi}{I_{zz}} \quad (44)$$

Integrating once will give us $(p, q, r)^T$.

Then using $\nu = \omega_\eta \dot{\eta}$ we can calculate $(\phi\ \theta\ \psi)^T$

$$\begin{bmatrix} \dot{p} \\ \dot{q} \\ \dot{r} \end{bmatrix} (\omega_\eta^{-1}) + \begin{bmatrix} p \\ q \\ r \end{bmatrix} \frac{d}{dt}(\omega_\eta^{-1}) = \begin{bmatrix} \dot{\phi} \\ \dot{\theta} \\ \dot{\psi} \end{bmatrix} \quad (45)$$

Integrating $[\dot{\phi}\ \dot{\theta}\ \dot{\psi}]^T$ we will get $[\phi\ \theta\ \psi]^T$.

CHAPTER IV

CONTROL DESIGN

In the following chapter, a PID Controller has been designed for controlling the altitude and position of the hexacopter.

Before designing the controller, a simple PID Controller is discussed:

PID Controller: The function of a controller is to control the dynamic system [30]. Its objective is to get the desired output from a system maintaining the stability of the system.

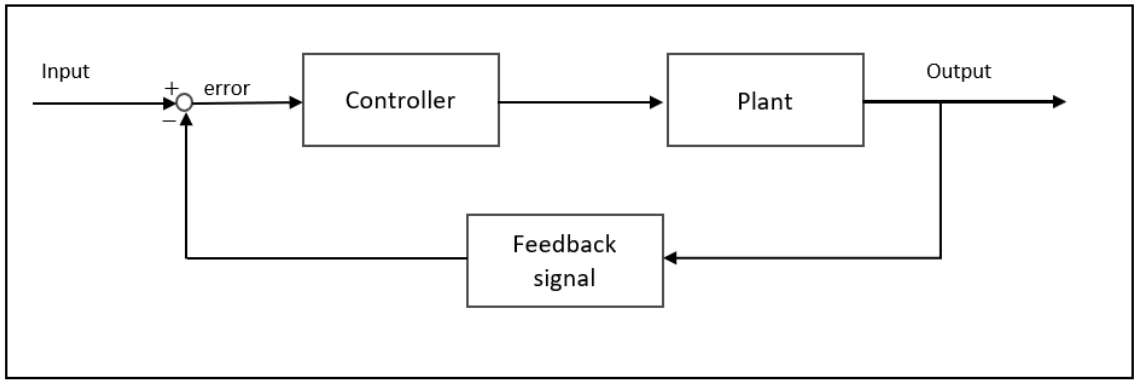

Figure 15. The functioning of a Controller

Different Controllers:

- PI controller
- PD controller
- PID controller

PI Controller: In the P Controller an offset exists between the process variable and set point and to overcome that I controller is added to the P controller [30]. In PI controller the controller multiplies the error by gain K_p and then adds the integral term of error to the proportional. The I

integrates the error over a period of time to give zero error value.

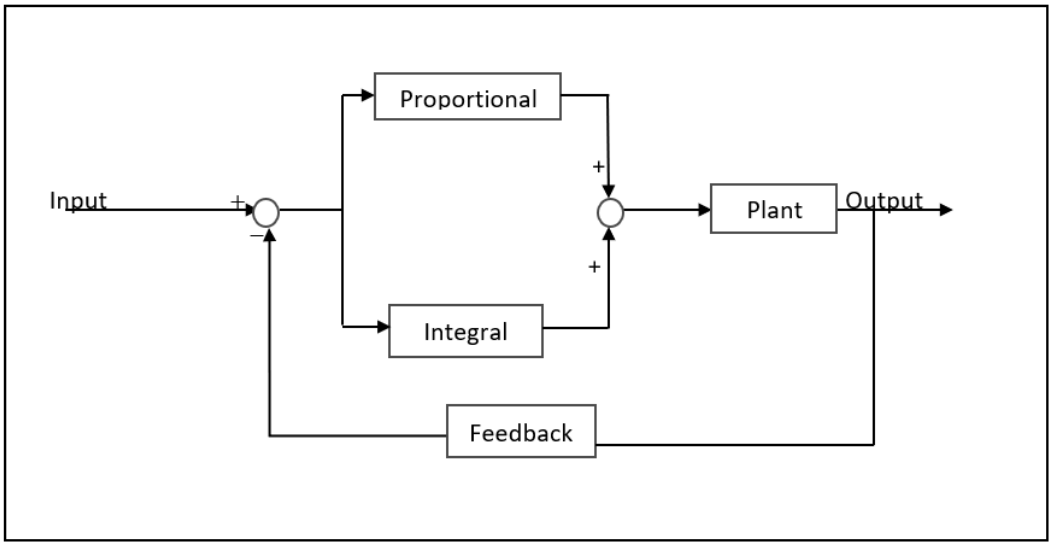

Figure 16. PI Controller

PD Controller: The PI Controller cannot predict the future of the kind of error which could occur, so Derivate controller or D controller is used to overcoming this problem as the derivative controller can anticipate the future behavior of the error [30]. It decreases the settling time and increases the system response. In PD Controller the controller multiplies the error by gain Kp and adds the integral value of the error of the derivative term.

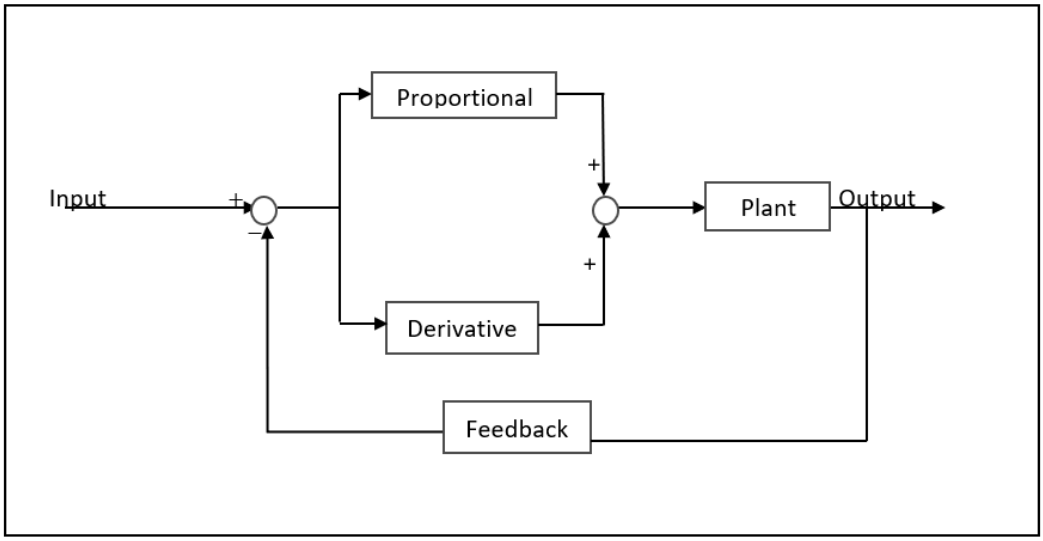

Figure 17. PD Controller

PID Controller: The PID consists of 3 terms the Proportional, the Integral and the Derivative. Combined actions of all three controllers give the best-stabilized control results [30]. The PID Controller is more stable compared to the rest of controllers, it has no steady state error and gives low maximum overshoot.

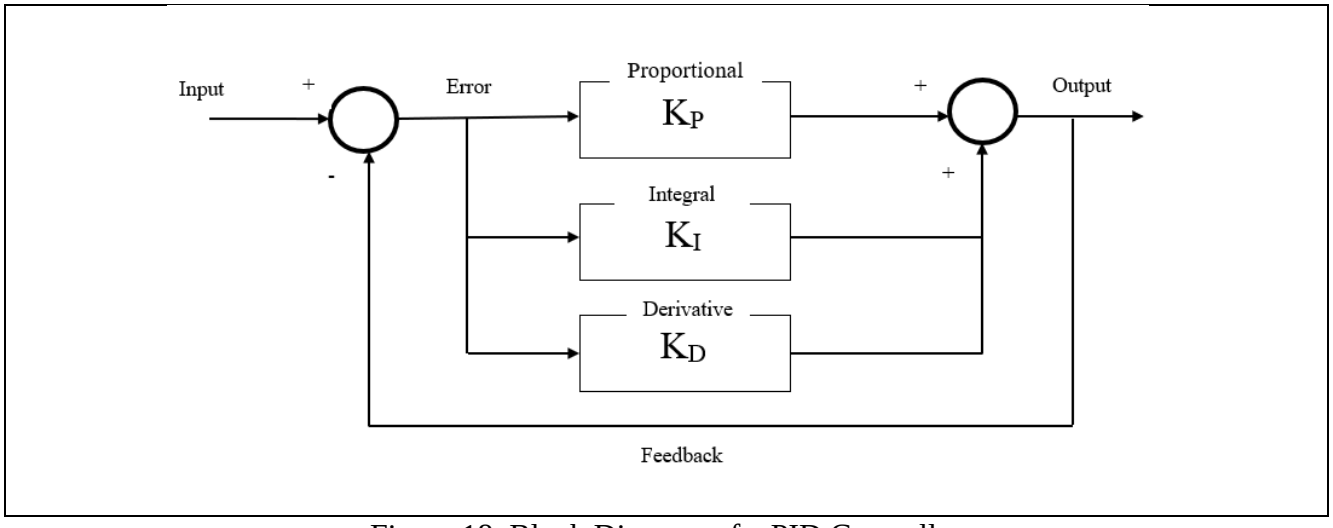

Figure 18. Block Diagram of a PID Controller

Tuning methods of PID Controller:

Before the PID Controller starts working, it needs to be tuned according to the dynamics and nature of the process which it will be controlling [31]. Although the default values for P, I and D terms are given by the designers, these values do not always suit the requirements of the operator and can lead to overshoot and steady-state error in the system. To overcome these different tuning methods are given to tune the PID Controllers which require as much attention as is given during the designing of the controller. Some of the tuning methods are discussed below.

Trial and Error Method:

In this method, the K_i and K_d values are set to zero and the proportional gain value K_p is increased until the system reaches oscillating behavior [31]. Once the system starts oscillating, the K_i values are adjusted to stop the oscillations and then the final step is to adjust K_d to get a fast response.

Zeigler-Nichols Method: In the Zeigler-Nichols method first, the value of K_P is set to a constant value first and K_i, K_d values are set to zero [31]. Proportional gain is increased until the system starts oscillating at a constant amplitude. Once this is reached, Zeigler-Nichols table can be used to enter the values of P, I and D in the PID controller.

Table 1. Zeigler-Nichols Table [31]

	K_p	T_I	T_D
P	$K_{pu}/2$	infinity	0
PI	$K_{pu}/2.2$	$P_u/1.2$	0
PID	$K_{pu}/1.7$	$P_u/2$	$P_u/8$

Process reaction curve technique: It uses the step input to produce a response in the system [31]. The Operator has to apply some control output to the system manually and then have to record the response curve. After getting the response curve we need to calculate values of dead time, slope, rise time for the curve and then substitute these values in P, I and D equations to get gain values of the desired terms.

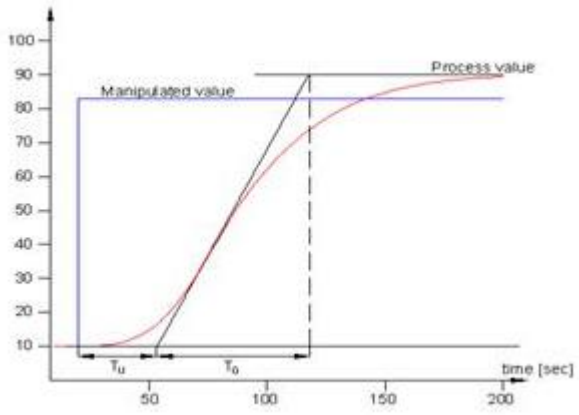

Figure 19. Process reaction curve [31]

4.1 Controller Design (new work)

This section presents the control of the hexacopter. The hexacopter is controlled by adjusting its angular velocities which are spun by electric motors. Its stabilization has been achieved by using the PD controller which is simple and easy to implement. From [32], the controller for a hexacopter is presented in this work. A simple examining method is developed to control the path or trajectory of the hexacopter flight. Then a PD controller is integrated to reduce the effect of oscillations or fluctuations in the flight behavior which can be caused by random external factors. The general form of the PD controller is given by:

$$e(t) = x_d(t) - x(t)$$

$$u(t) = K_p e(t) + K_D \frac{de(t)}{dt} \tag{46}$$

where u(t) is the output for control, x_d is for the desired position, x(t) is the present state and K_D and K_p are the parameters for the derivative and proportional elements of PD controller. The interactions between the total thrust T, total torque τ generated by the rotors can be seen from the hexacopter dynamics in equations (15), (16), and (30). The total thrust influences the acceleration in the z-direction and holds the hexacopter in the air. Torque $\tau\theta$ has an effect on the acceleration of angle θ, $\tau\phi$ effects the acceleration of angle ϕ and $\tau\varphi$ effects the acceleration of angle φ.

The equations for total thrust T and torques can be written as:

$$T = (g + K_{z,D}(\dot{z}_d - \dot{z}) + K_{Z,P}(z_d - z))\frac{m}{C\phi C\theta}, \tag{47}$$

$$\tau\phi = (K_{\phi,D}(\dot{\phi}_d - \dot{\phi}) + K_{\phi,P}(\phi_d - \phi))I_{xx},$$

$$\tau\theta = (K_{\theta,D}(\dot{\theta}_d - \dot{\theta}) + K_{\theta,P}(\theta_d - \theta))I_{yy},$$

$$\tau\varphi = (K_{\psi,D}(\dot{\psi}_d - \dot{\psi}) + K_{\psi,P}(\psi_d - \psi))I_{zz},$$

where mass m, gravity g and moment of inertia I of the hexacopter are also considered.

The angular velocities of rotors ω_i can be calculated from equations (30) and (47)

$$\omega_1^2 = \frac{T}{6k} - \frac{2\tau\theta}{5kl} - \frac{\tau\varphi}{10b}, \tag{48}$$

$$\omega_2^2 = \frac{T}{6k} + \frac{\tau\phi}{3kl} - \frac{\tau\theta}{5kl} + \frac{\tau\varphi}{5b},$$

$$\omega_3^2 = \frac{T}{6k} + \frac{\tau\phi}{3kl} + \frac{\tau\theta}{5kl} - \frac{\tau\varphi}{5b},$$

$$\omega_4^2 = \frac{T}{6k} + \frac{2\tau\theta}{5kl} + \frac{\tau\varphi}{10b},$$

$$\omega_5^2 = \frac{T}{6k} - \frac{\tau\phi}{3kl} + \frac{\tau\theta}{5kl} - \frac{\tau\varphi}{5b},$$

$$\omega_6^2 = \frac{T}{6k} - \frac{\tau\phi}{3kl} - \frac{\tau\theta}{5kl} + \frac{\tau\varphi}{5b}$$

where k is the lift constant, b is the drag constant and l is the distance between the center of gravity of the hexacopter and the rotor.

Table 2. Parameter values considered for simulation

Parameter	Value	Unit
gravity	9.81	m/s^2
mass	2.468	Kg
length	0.225	m
k	2.980e-6	-
b	1.140e-7	-
I_{xx}	4.856e-3	kgm^2
I_{yy}	4.856e-3	kgm^2
I_{zz}	8.801e-3	kgm^2
I_r	3.357e-5	kgm^2

The proportional and derivative parameter values considered for the PD controller are given below.

Table 3. Parameter values for the PD Controller

Parameter	Value	Parameter	Value
$K_{Z,D}$	2.20	$K_{Z,P}$	3.75
$K_{\phi,D}$	3.75	$K_{\phi,P}$	10
$K_{\theta,D}$	3.75	$K_{\theta,P}$	10
$K_{\psi,D}$	3.75	$K_{\psi,P}$	10

The performance of the controller is tested with different input of angles (roll, pitch, yaw) and position (x, y, and z). The parameter values are chosen on the basis of trial and error. First, the value of proportional is inserted keeping the value of derivative as zero and then the derivative value is selected on the basis of trial and error. The angles are stabilized to the given input in under ten seconds which shows that the hexacopter is able to control the movements of roll, pitch, and yaw. The graphs showing the final results are presented in the next chapter.

CHAPTER V

SIMULATION AND RESULTS

This chapter focuses on the results and simulations generated from the Proportional and Derivative controller and shows how the hexacopter would behave at the different input of angles for the Roll, Pitch, and Yaw. Different cases were taken, and graphs were generated which represent the angles (Roll, Pitch, and Yaw) and positions (x, y, and z) of the hexacopter.

Case1.

Roll Angle Active: In this case, an input of Roll (Phi) is given to the system and the response is simulated. The system is tested for two different values of Roll, given in radians. Also, the angles in Pitch and Yaw remain inactive during this case.

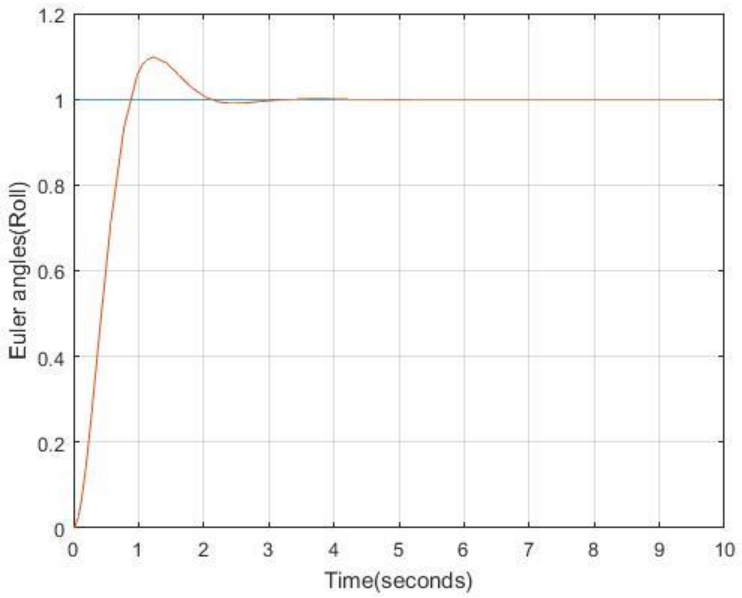

Figure 20. Roll angle measured in radians for a value of 1

Figure 20 represents roll angle vs time. From the figure, it can be observed that the system attains zero steady-state error in less than 5 seconds. The overshoot of the system also remains small.

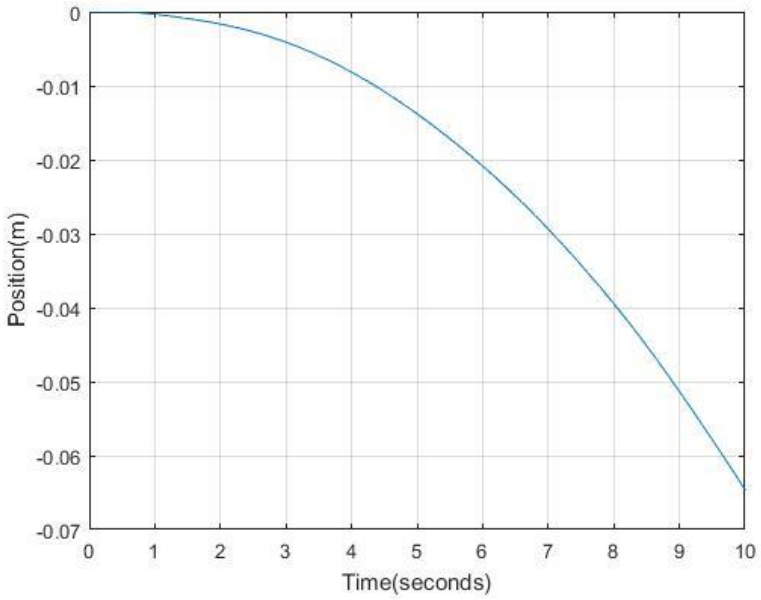

Figure 21. Effect of Roll angle on y-position for a value of 1

Figure 21 represents the effect of roll angle on the position of the hexacopter. When an input for roll angle is given the hexacopter reacts by rolling towards the desired angle and while rolling there is a minor effect in the position in the y-direction. In this case, an input of 1 radian is given and the hexacopter reacts by going 0.07m in the negative y-direction.

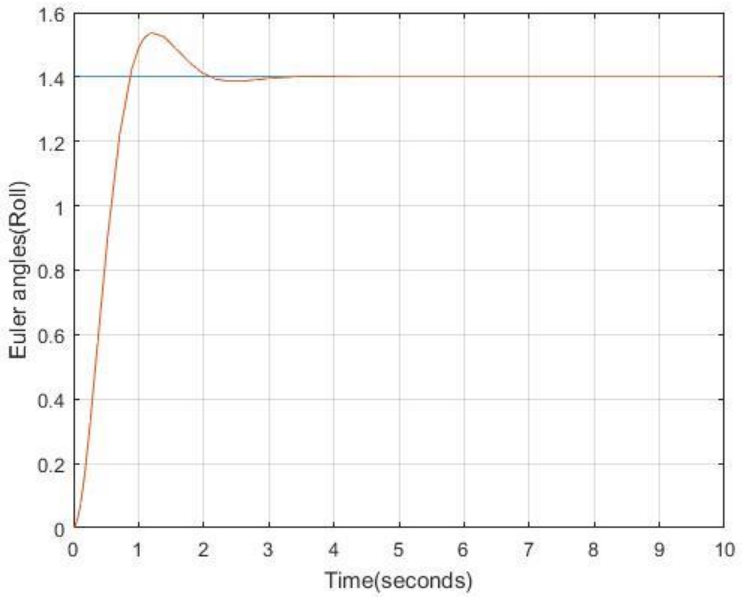

Figure 22. Roll angle measured in radians for a value of 1.4

Figure 22 represents the system response to an input of 1.4 radians as Roll. From the figure, it is observed that the system attains zero steady-state error in less than 4 seconds.

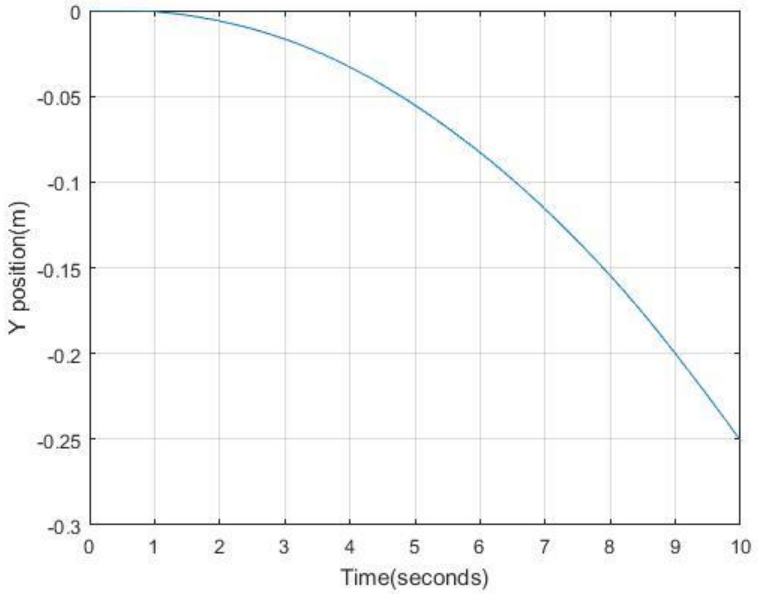

Figure 23. Effect of Roll angle on y-position for a value of 1.4

Figure 23 represents the effect of roll angle on the position of the hexacopter. When an input for roll angle is given in radians the hexacopter reacts by rolling towards the desired angle and while rolling there is a minor change in the position in the y-direction. In this case, an input of 1.4 radians is given and the hexacopter reacts by going 0.25m in the negative y-direction.

Case2.

Pitch Angle Active: In this case, an input of Pitch (Theta) is given to the system and the response is simulated. The system is tested for two different values of Pitch, given in radians. Also, the angles in Roll and Yaw remain inactive during this case.

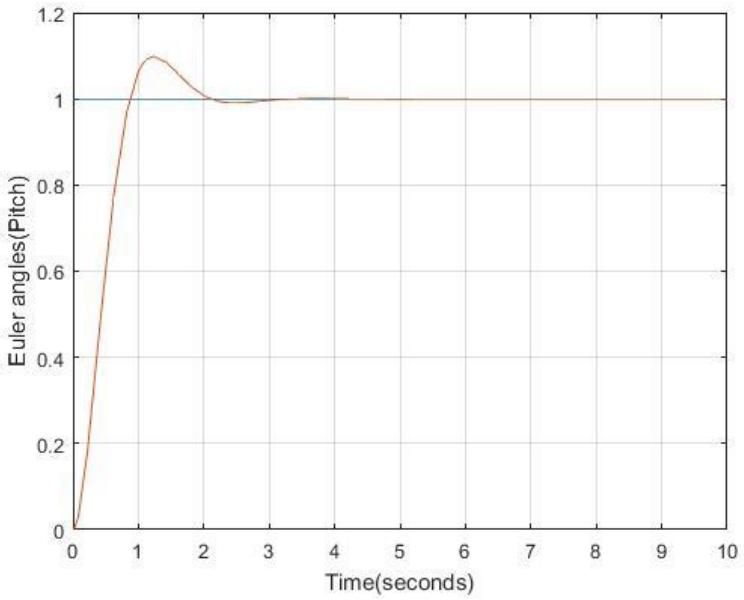

Figure 24. Pitch angle measured in radians for a value of 1

Figure 24 represents pitch angle vs time. From the figure, it can be observed that the system attains zero steady-state error in less than 5 seconds. The overshoot of the system also remains small.

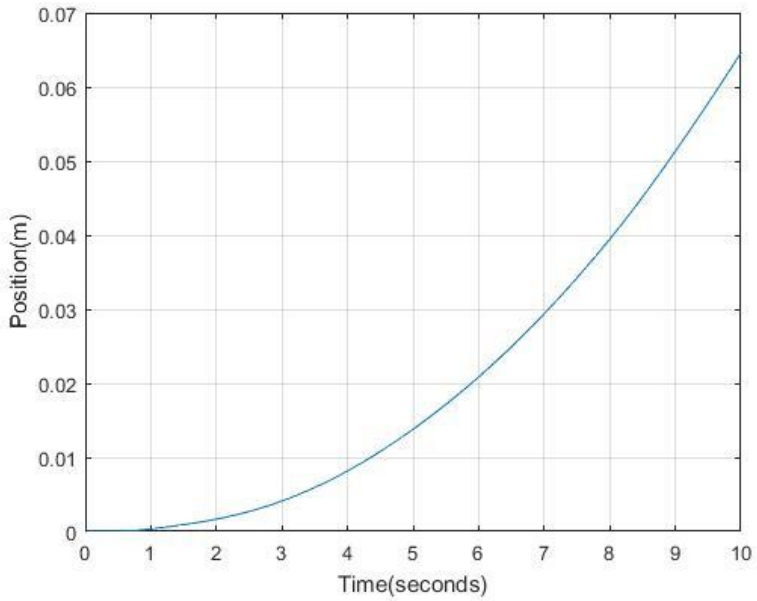

Figure 25. Effect of Pitch angle on x-position for a value of 1

Figure 25 represents the effect of pitch angle on the position of the hexacopter. When an input for pitch angle is given the hexacopter reacts by pitching towards the desired angle and while pitching there is an effect in the x-direction. In this case, an input of 1 radian is given and the hexacopter reacts by going 0.07m in the positive x-direction and a graph between x-position and time is plotted.

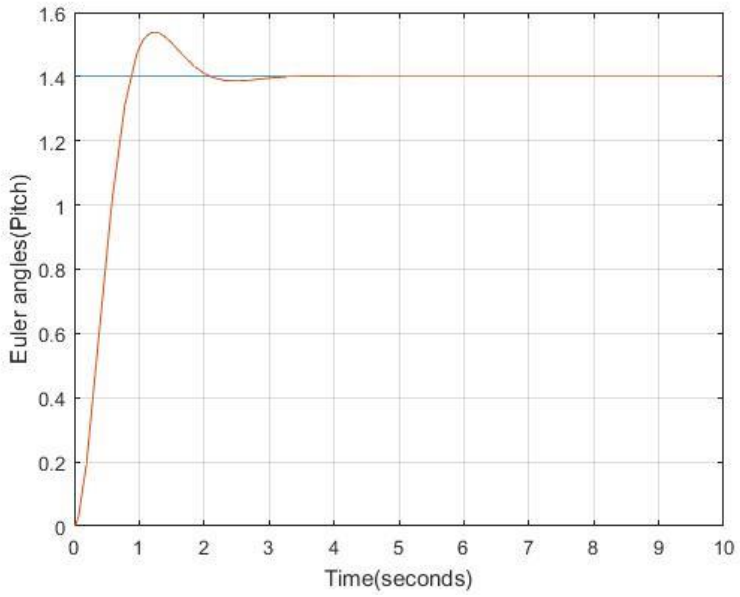

Figure 26. Pitch angle measured in radians for a value of 1.4

Figure 26 represents the system response to an input of 1.4 radians as Pitch. From the figure, it is observed that the system attains zero steady-state error in less than 4 seconds.

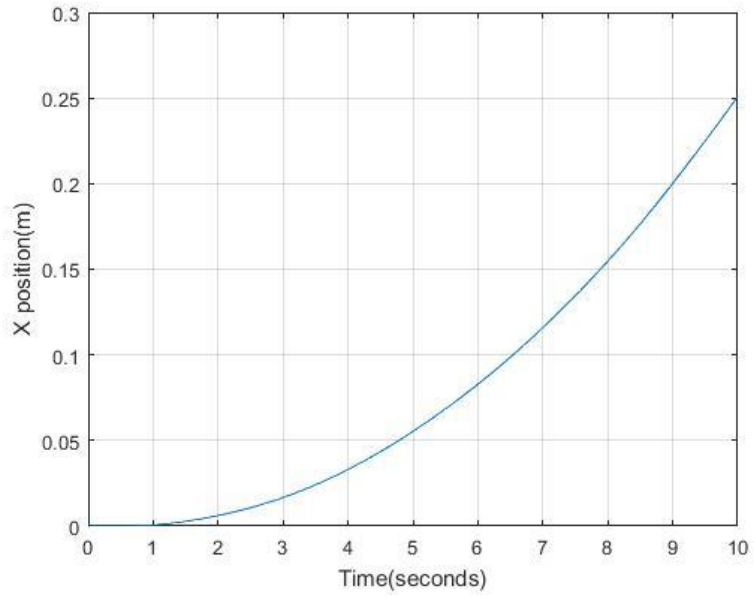

Figure 27. Effect of Pitch angle on x-position for a value of 1.4

Figure 27 represents the effect of pitch angle on the position of the hexacopter. When an input for pitch angle is given the hexacopter reacts by pitching towards the desired angle and while pitching there is a minor change in the position in the x-direction. In this case, an input of 1.4 radians is given and the hexacopter reacts by going 0.25m in the positive x-direction.

Case3.

Yaw Angle Active: In this case, an input of Yaw (Psi) is given to the system and the response is simulated. The system is tested for two different values of Yaw, given in radians. Also, the angles in Roll and Pitch remain inactive during this case.

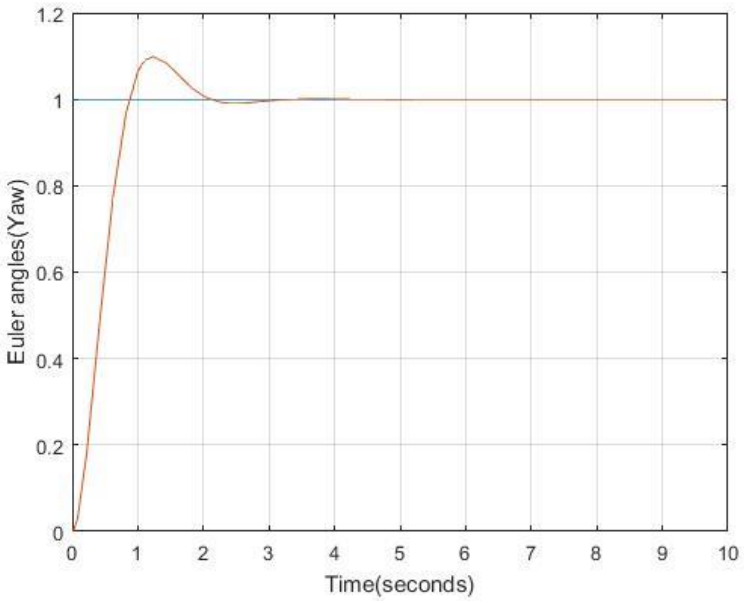

Figure 28. Yaw angle measured in radians for a value of 1

Figure 28 represents yaw angle vs time. From the figure, it can be observed that the system attains zero steady-state error in less than 5 seconds. The overshoot of the system also remains small. In the case of yawing, angular velocities ω_1, ω_3 and ω_5 act in one direction and angular velocities ω_2, ω_4 and ω_6 act in opposite direction. In the case of yawing, there is no change in the position of x and y and the hexacopter hovers at one position.

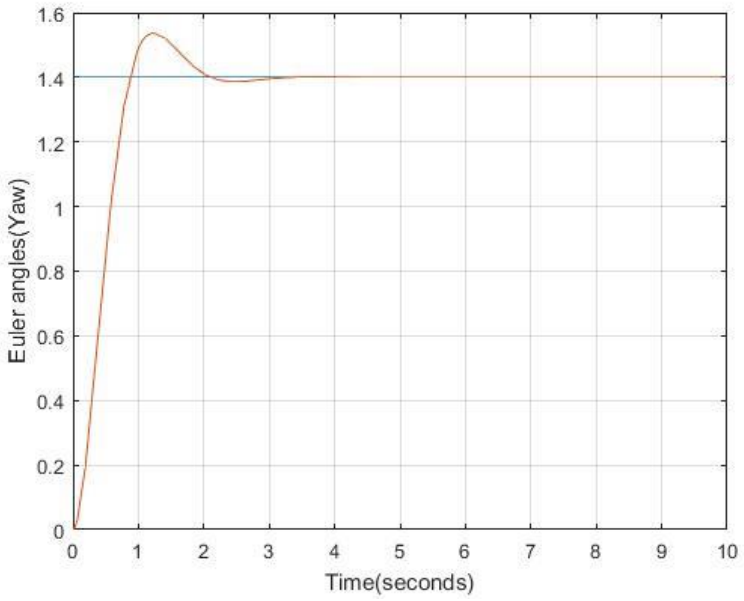

Figure 29. Yaw angle measured in radians for a value of 1.4

Figure 29 represents the system response to an input of 1.4 radians as Yaw. From the figure, it is observed that the system attains zero steady-state error in less than 4 seconds. In the case of yawing, angular velocities ω_1, ω_3 and ω_5 act in one direction and angular velocities ω_2, ω_4 and ω_6 act in opposite direction. In the case of yawing, there is no change in the position of x and y and the hexacopter hovers at one position.

Case4.

A separate controller is designed to control the altitude (z-position) of the hexacopter and a graph between z-position and time is plotted.

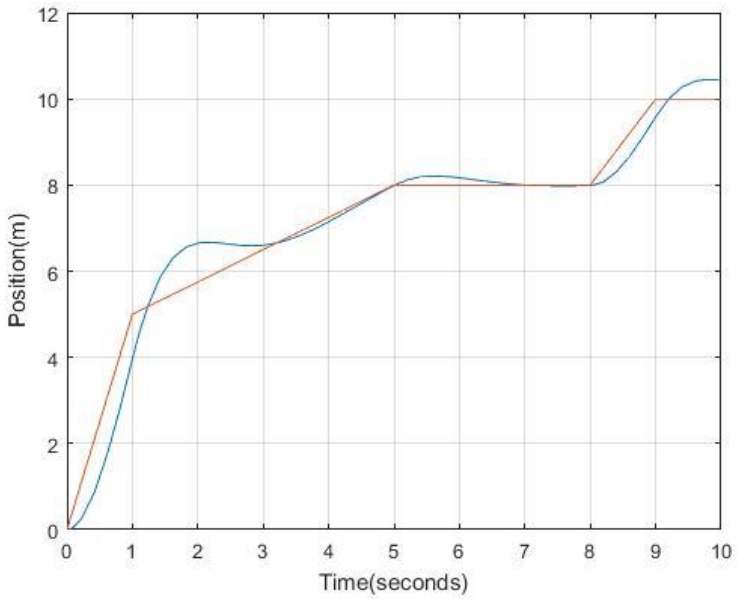

Figure 30. z-position vs time graph

Figure 30 represents altitude (z-position) vs time. A separate controller is designed to control the altitude of the hexacopter. In the above graph, the hexacopter follows a given path which is given using a signal builder. The hexacopter reaches a height of five meters in one second and then gradually increases and reaches a height of eight meters in five seconds then it stays at eight meters for three seconds before going up to a height of ten meters. As seen from the Figure, the hexacopter is to reach an altitude of 10m in a short interval of time, hence, a small overshoot is observed.

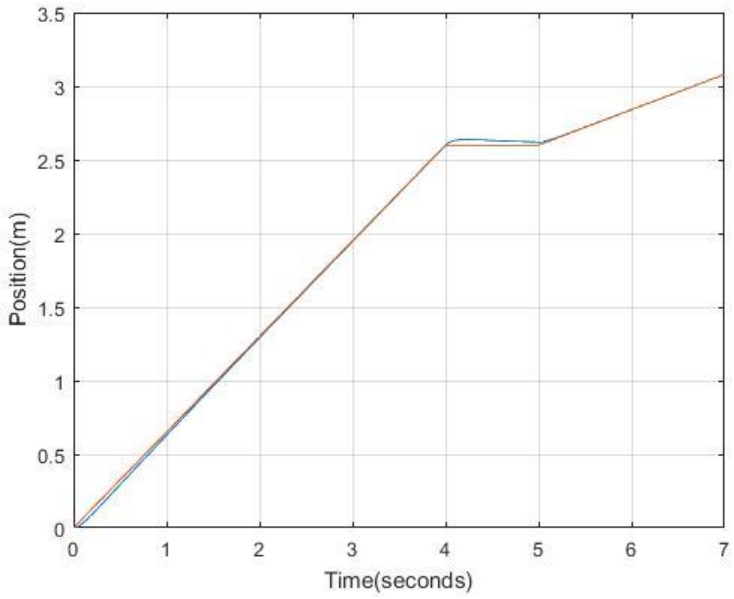

Figure 31. z-position vs time graph

Figure 31 represents altitude (z-position) vs time. In the above graph, the hexacopter follows a given path which is given using a signal builder. The hexacopter reaches a height of 2.6 meters in four seconds, it stays at 2.6m for a second and then gradually increases and reaches a height of 3.1m in seven seconds. The graph has no overshoot and sufficiently small steady-state error as the hexacopter is given more time to attain the required height.

Case 5.

Figures 32, 33 and 34 represent the roll angle vs time, the pitch angle vs time, and the yaw angle vs time graphs respectively after the introduction of external disturbances to the system. The PD values were altered to get the desired results for the flight.

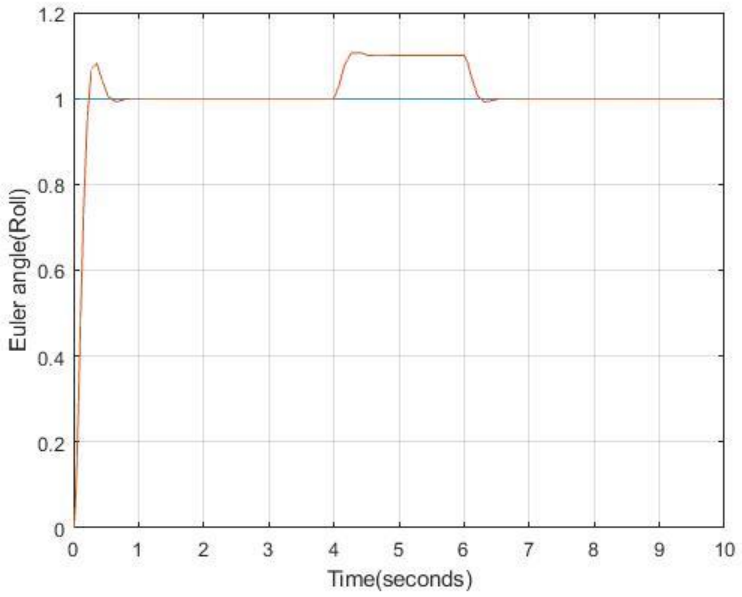

Figure 32. Roll angle vs Time graph

Figure 32 represents roll angle vs time graph for a value of one radian in the presence of external disturbances applied between 4 and 6 seconds which can affect the flight of the hexacopter. It can be seen from the graph, that the controller rejects the disturbance effectively and provides the hexacopter to follow the desired path.

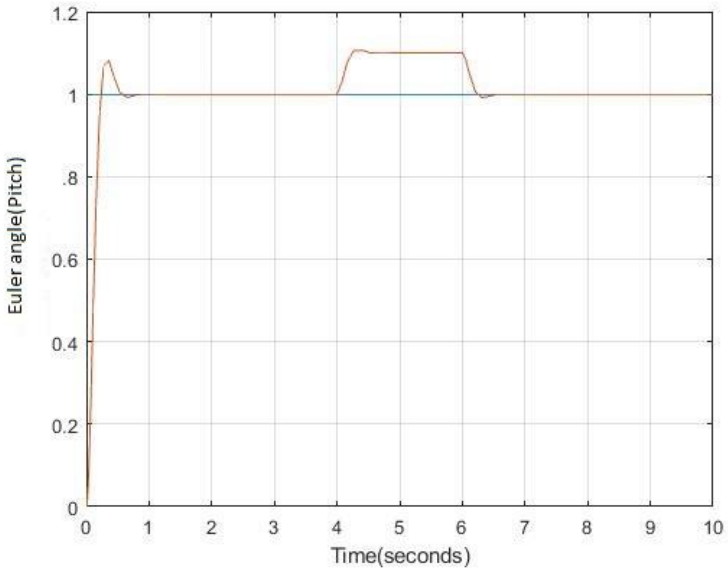

Figure 33. Pitch angle vs Time graph

Figure 33 represents pitch angle vs time graph for a value of one radian in the presence of external disturbances applied between 4 and 6 seconds which can affect the flight of the hexacopter. It can be seen from the graph, that the controller rejects the disturbances effectively and provides the hexacopter to follow the desired path.

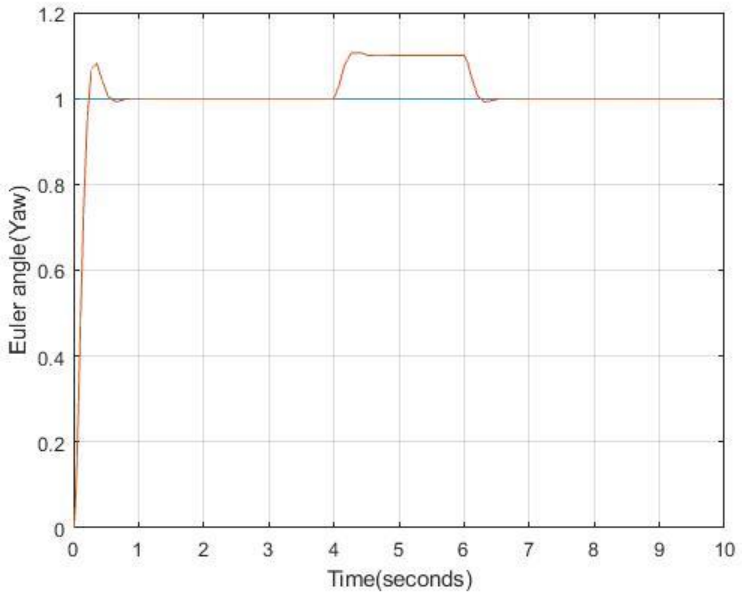

Figure 34. Yaw angle vs Time graph

Figure 34 represents yaw angle vs time graph for a value of one radian in the presence of external disturbances applied between 4 and 6 seconds which can affect the flight of the hexacopter. It can be seen from the graph, that the controller rejects the disturbance effectively and provides the hexacopter to follow the desired path.

A comparison between Quadcopters, Hexacopters and, Octocopters based on price, complexity, motors, payload, power, stability and size has been shown in the table below.

Table 4. Comparison between Quadcopter, Hexacopter, and Octocopter

	Quadcopter	Hexacopter	Octocopter
Price	Cheapest compared to a hexacopter and an octocopter.	Expensive than a Quadcopter but cheaper than an Octocopter.	Most expensive.
Complexity	Very easy to build as it has the least complex design.	More complex model than a quadcopter, harder to build but less complex than an octocopter.	Most complex model, very hard to build.

Table 4. Continued…

	Quadcopter	Hexacopter	Octocopter
Motor	Does not have backup motors.	Has backup motors to support motor failure.	Has backup motors to support motor failure.
Payload	Cannot carry heavy payloads.	Can carry heavy payloads.	Can carry heavy payloads.
Power	Least powerful drone as compared to the hexacopter and the octocopter.	More powerful drone compared to a quadcopter but less powerful compared to an octocopter.	Most powerful drone as compared to a quadcopter or a hexacopter.
Stability	A quadcopter is not as stable as the hexacopter and the octocopter.	More stable than a quadcopter but less stable than an octocopter.	Most stable drone.
Size	Smaller in size as compared to the hexacopter and the octocopter.	Bigger in size than a quadcopter but smaller than an octocopter.	Biggest in size.

CHAPTER VI

CONCLUSION AND FUTURE WORK

6.1 Conclusion:

The purpose of this thesis was to study the Modeling and Controls of a Hexacopter. The differential equations for the hexacopter were derived using the Newton-Euler method and the mathematical model was discussed. All the equations for the translational force, the rotational force, and the moment were mentioned in detail. Based on the equations, a mathematical model was designed for the hexacopter and equations for the acceleration were derived in the body frame and the inertial frame. Different tuning methods for tuning a PID controller were studied and simple block diagrams for different types of PID controllers were made and studied. Based on the mathematical model a controller was designed for the hexacopter and was tested using the Matlab/Simulink.

A Proportional and Derivative Controller (PD Controller) has already been designed for the controls of a Quadcopter but it has never been implemented for a Hexacopter. In this thesis, a proportional and derivative controller was studied and designed for a hexacopter for controlling the altitude and attitude of the hexacopter and was tested for different attitudes and altitudes. The model was then verified using Simulink to simulate the flight of the hexacopter. The simulation graphs were generated and studied considering different cases of angles (Roll, Pitch, and Yaw). In the first case, graphs for the roll angle were plotted for two different values of angles and were studied. In the second case, graphs for pitch angle were generated and studied for two different cases of angles. In the third case, graphs for yaw angle were generated for two different values of angles and were studied. The simulation proved the described model to be practical in modeling the attitude, altitude, and position of the hexacopter. Further, the

simulation results also showed that the PD controller was enough in stabilizing the hexacopter to the required altitude and attitude for the given input. In the fourth case, graphs between altitude and time for two different altitudes were plotted and studied. In the first of the two cases, hexacopter was asked to reach a higher altitude in short span of time and in the second case the hexacopter was given enough time to reach the given altitude and the graphs for both the cases were generated and results were studied.

A separate proportional and derivative controller was also designed for tackling external disturbances and the results were simulated using Simulink. The simulation results were discussed for all the three angles. The external disturbances were introduced to the system from four seconds to six seconds and the controller showed a small overshoot during that time but overall the results showed that the hexacopter can overcome the disturbances easily and still follow the desired path for the given input of angles. The results were only generated using the proportional and derivative controller, the integral part of the PID controller was not introduced. Moreover, the results were not tested using the real physical model of the hexacopter.

A comparison between Quadcopters, Hexacopters, and Octocopters was also done based on various parameters like price, structure, payload, power, size, stability, and motor and the results were added in a table format.

6.2 Future Work:

Future work will include testing the hexacopter at more angles and working on increasing the hovering time. Working to include an integral along with the proportional and derivative part of the controller. Moreover, improvisation of the controller can also be done to perform various tasks like avoiding barriers, weather forecasting, traffic control, pick and place etc. The electric motors used for spinning the six rotors were not modeled and the results were only

tested using Simulink. A real hexacopter prototype should be constructed and tested using these simulation results to accomplish more realistic results. Further modifications can be made in the controller to reduce the minor overshoot which occurs during the presence of external factors to have a smoother flight of the hexacopter.

REFERENCES

[1] V. Artale, C. Milazzo and A. Ricciardello, "Mathematical modeling of hexacopter", Applied Mathematical Sciences, vol. 7, pp. 4805-4811, 2013.

[2] J. Ligthart, P. Poksawat, L. Wang and H. Nijmeijer, "Experimentally Validated Model Predictive Controller for a Hexacopter. The authors gratefully acknowledge the partial sponsorship by DSTG, Australia.", IFAC-PapersOnLine, vol. 50, no. 1, pp. 4076-4081, 2017.

[3] M. Moussid, A. Sayouti and H. Medromi, "Dynamic Modeling and Control of a HexaRotor using Linear and Nonlinear Methods", International Journal of Applied Information Systems, vol. 9, no. 5, pp. 9-17, 2015.

[4] A. Alaimo, V. Artale, C. Milazzo, and A. Ricciardello, "PID Controller Applied to Hexacopter Flight", Journal of Intelligent & Robotic Systems, vol. 73, no. 1-4, pp. 261-270, 2013.

[5] Morales, Camilo, Diana Ovalle, and Alain Gauthier. "Hexacopter maneuverability capability: An optimal control approach." Modeling, Simulation, and Applied Optimization (ICMSAO), 2017 7th International Conference on. IEEE, 2017.

[6] Falconí, Guillermo P., Christian D. Heise, and Florian Holzapfel. "Fault-tolerant position tracking of a hexacopter using an Extended State Observer." Automation, Robotics, and Applications (ICARA), 2015 6th International Conference on. IEEE, 2015.

[7] Ahmed, O. A., et al. "Stabilization and control of autonomous hexacopter via visual-servoing and cascaded-proportional and derivative (PD) controllers." Automation, Robotics, and Applications (ICARA), 2015 6th International Conference on. IEEE, 2015.

[8] Baránek, Radek, and František Šolc. "Modeling and control of a hexacopter." Carpathian Control Conference (ICCC), 2012 13th International. IEEE, 2012.

[9] Leishman, Robert, et al. "Relative navigation and control of a hexacopter." Robotics and Automation (ICRA), 2012 IEEE International Conference on. IEEE, 2012.

[10] E. Bekir, Introduction to modern navigation systems. Singapore: World Scientific, 2007.

[11] D. Küchemann, Progress in aerospace sciences, vol. 12. Pergamon Pr., 1972.

[12] D. Wang, "Quadcopter Parts: What are they and what do they do? – Quadcopter Academy", Quadcopter Academy, 2017. [Online]. Available: http://www.quadcopteracademy.com/quadcopter-parts-what-are-they-and-what-do-they-do/. [Accessed: 24- Nov- 2017].

[13] "Components of a Multirotor - Drones and Multirotors: Types, Components & Uses", Sites.google.com, 2017. [Online]. Available: https://sites.google.com/a/ewg.k12.ri.us/drones-types-components-and-uses/home/components-of-a-multirotor. [Accessed: 24- Nov- 2017].

[14] Ae01.alicdn.com, 2017. [Online]. Available: https://ae01.alicdn.com/kf/HTB1YRgDKpXXXXaPXXXXq6xXFXXXu/Hexacopter-Drone-Brushless-Motor-450-Rc-F450-Quadcopter-Motor-Motors-Diy-Quadcopter-Drone-Parts-Set-Part.jpg_640x640.jpg. [Accessed: 26- Nov- 2017].

[15] I2.wp.com, 2017. [Online]. Available: https://i2.wp.com/www.americandronesonline.com/wp content/uploads/2016/07/182435a99cb1.jpg?fit=500%2C343 [Accessed: 26- Nov- 2017].

[16] Pisces.bbystatic.com, 2017. [Online]. Available: https://pisces.bbystatic.com/image2/BestBuy_US/images/products/4872/4872301_sd.jpg;maxHeight=640;maxWidth=550. [Accessed: 26- Nov- 2017].

[17] P. Michal Mazur, "Six Ways Drones Are Revolutionizing Agriculture", MIT Technology

Review, 2017. [Online]. Available: https://www.technologyreview.com/s/601935/six-ways-drones-are-revolutionizing-agriculture/. [Accessed: 26- Nov- 2017].

[18] Robotshop.com, 2017. [Online]. Available: http://www.robotshop.com/media/files/images2/tarot-960-folding-carbon-fiber-hexacopter-frame-large.jpg. [Accessed: 26- Nov- 2017].

[19] Bhphotovideo.com, 2017. [Online]. Available: https://www.bhphotovideo.com/images/images2500x2500/yuneec_yunh920034_4000mah_6cl_6s_22_2v_lpo_1223119.jpg. [Accessed: 26- Nov- 2017].

[20] NOVA, Rise of the Drones. (n.d.). [video] PBS [Accessed: September 20, 2018].

[21] Paul Pounds, Robert Mahony, Peter Corke, Modeling and Control of a Quad-Rotor Robot, Australian National University.

[22] Holger Voos, Nonlinear and Neural Network-based Control of a Small Four-Rotor Aerial Robot, IEEE, 2007.

[23] Bouabdallah, Samir, and Roland Y. Siegwart. "Full control of a quadrotor." IEEE/RSJ International Conference on Intelligent Robots and Systems, 2007: IROS 2007; Oct. 29, 2007-Nov. 2, 2007, San Diego, CA. Ieee, 2007.

[24] Pawar, A., Joshi, S., & Sulakhe, V. (2015). Development of Autopilot for VTOL application [Accessed: September 20, 2018].

[25] Salih, A. L., Moghavvemi, M., Mohamed, H. A., & Gaeid, K. S. (2010). Flight PID controller design for a UAV quadrotor. Scientific research and essays, 5(23), 3660-3667.

[26] Poksawat, P., & Wang, L. (2017, October). Automatic tuning of hexacopter attitude control systems with experimental validation. In 2017 21st International Conference on System Theory, Control and Computing (ICSTCC) (pp. 753-758). IEEE.

[27] Le, D. K., & Nam, T. K. (2015). A study on the modeling of a hexacopter. Korean Marine Engineering Journal, *39*(10), 1023-1030.

[28] Bose, S., Bagchi, A., & Dave, N. (2017). Hexacopter using MATLAB Simulink and MPU Sensing.

[29] Magnusson, T. (2014). Attitude control of a Hexarotor.

[30] Index of /Roboclub/Lectures, students.iitk.ac.in/roboclub/lectures [Accessed: September 20, 2018].

[31] "How Does a PID Controller Work? - Structure & Tuning Methods." ElProCus - Electronic Projects for Engineering Students, 2 Oct. 2014, www.elprocus.com/the-working-of-a-pid-controller/.

[32] Luukkonen, T. (2011). Modeling and control of quadcopter. Independent research project in applied mathematics, Espoo, 22.

APPENDIX A

MATLAB CODE

MATLAB Code:

```
Clear

Clf

close all

clc

% Start up for simulink file 'UAV_model'

Ixx=4.856*10^(-3);

Iyy=4.856*10^(-3);

Izz=8.801*10^(-3);

k=2.980*10^(-6); % Lift Constant

b=1.140*10^(-7); % Drag Constant

g=9.81; % Gravitation Constant

l=0.225; % Length

m=2.468; % Mass

Ir=3.357*10^(-5); % Inertial Moment of rotor

%kzd=2.20; kzp=3.75;

kzd=2.20; kzp=3.75;

kphip=10; kphid=3.75;

kthetad=3.75; kthetap=10;

kpsid=3.75; kpsip=10;

phi0=0;

theta0=0;

psi0=0;
```

```
z0=0;
[t,x,y]=sim('UAV_model',[0,10]);
figure(1),plot(t,y(:,1:2)),grid
figure(2),plot(t,y(:,3)),grid
figure(3),plot(t,y(:,4:5)),grid
figure(4),plot(t,y(:,6)),grid
figure(5),plot(t,y(:,7:8)),grid
figure(6),plot(t,y(:,9:10)),grid
figure(7),plot(t,y(:,11)),grid
sim('UAV_model',[0 10]);
% Simout= sim('UAV_model');
```

APPENDIX B

SIMULINK MODEL

Simulink model:

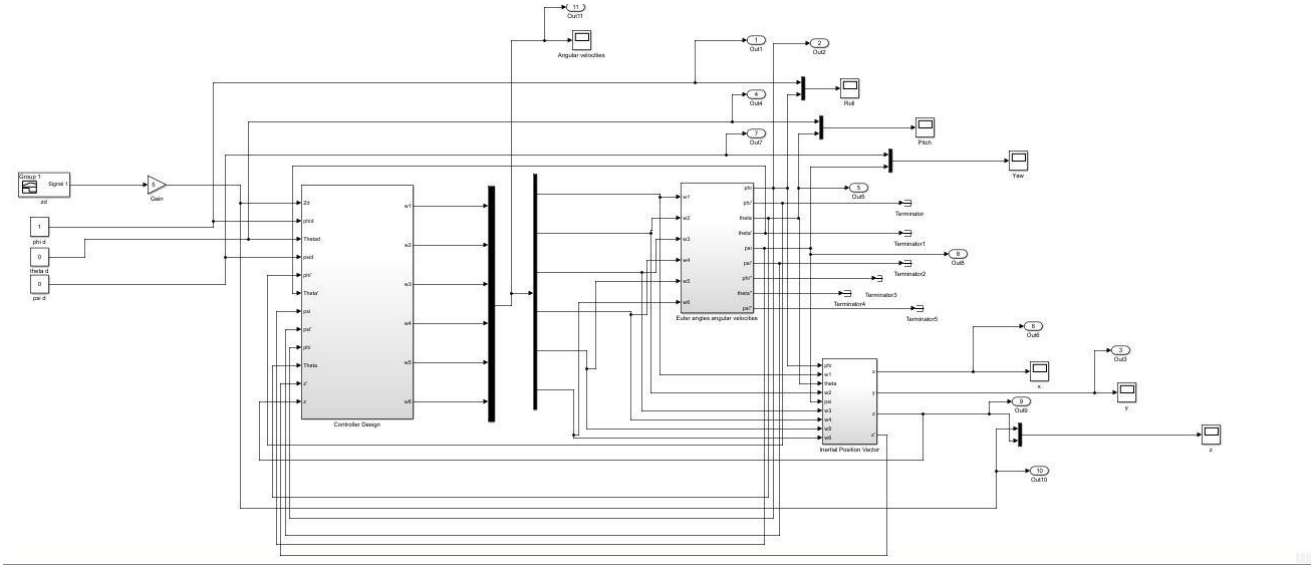

Figure B1. Simulink model

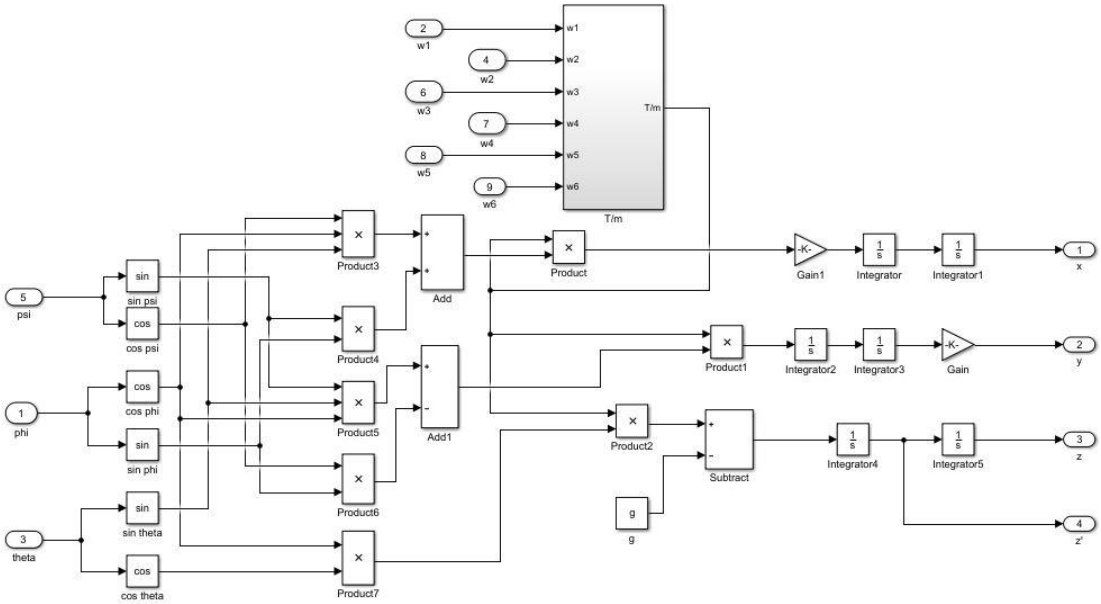

Figure B2. Inertial Position Vector

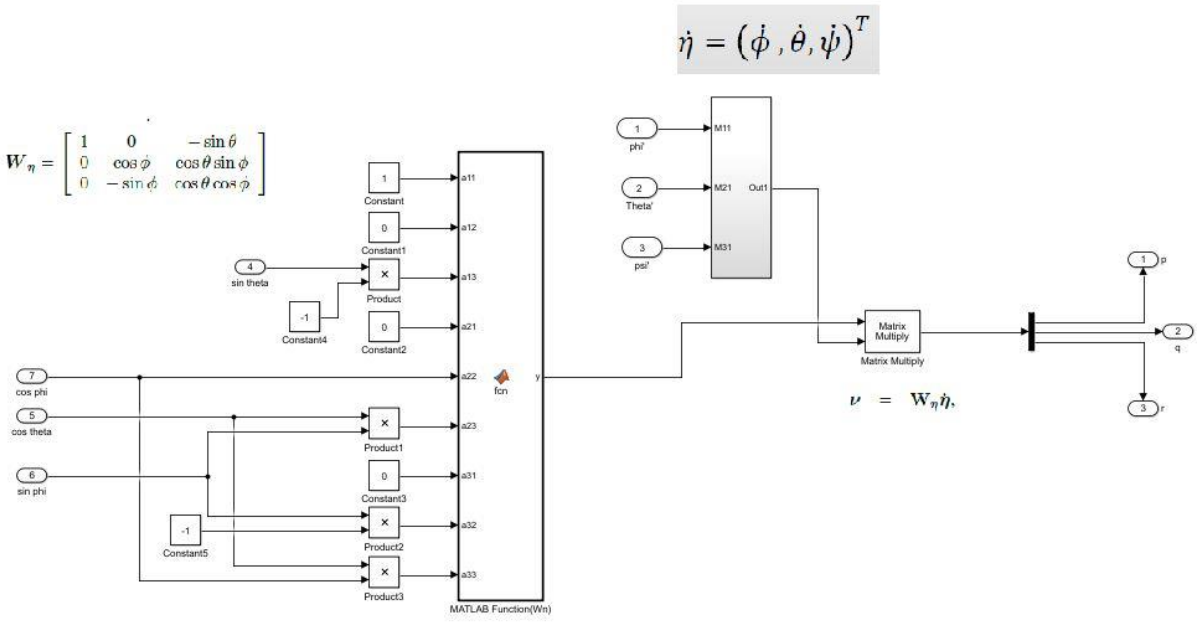

Figure B3. Angular Velocity Calculation

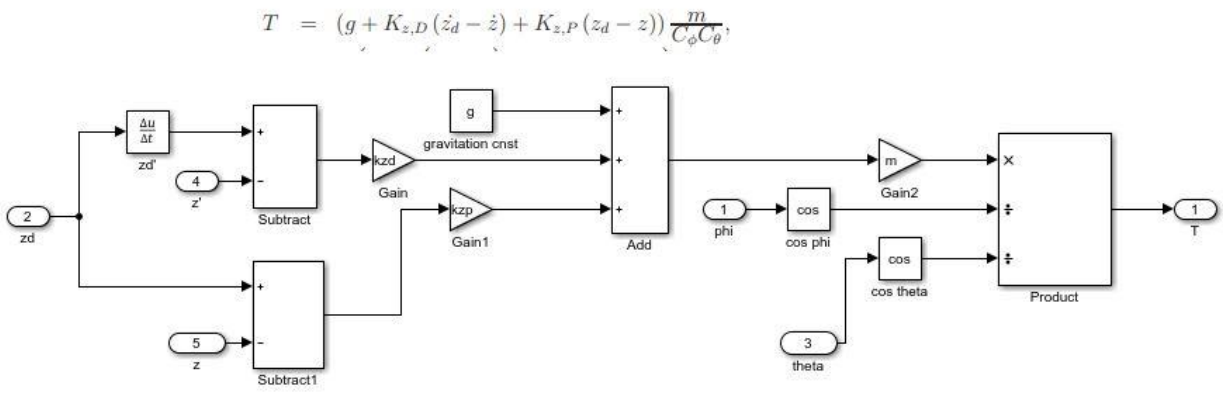

Figure B4. Altitude Control

$$\tau_\phi = \left(K_{\phi,D}\left(\dot{\phi}_d - \dot{\phi}\right) + K_{\phi,P}\left(\phi_d - \phi\right)\right) I_{xx},$$

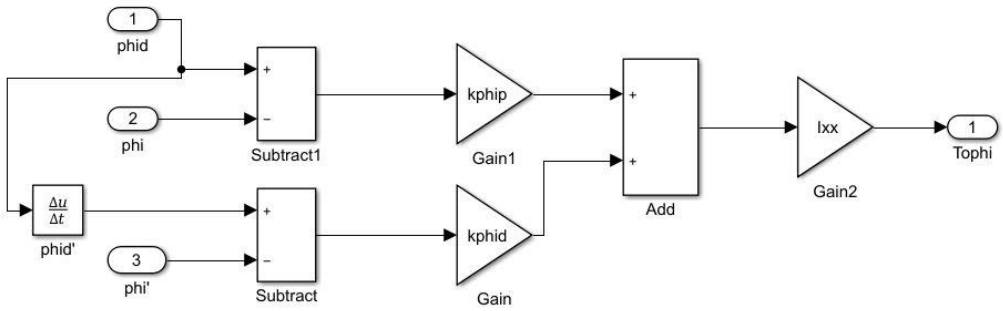

Figure B5. Roll Control

$$\tau_\theta = \left(K_{\theta,D}\left(\dot{\theta}_d - \dot{\theta}\right) + K_{\theta,P}\left(\theta_d - \theta\right)\right) I_{yy},$$

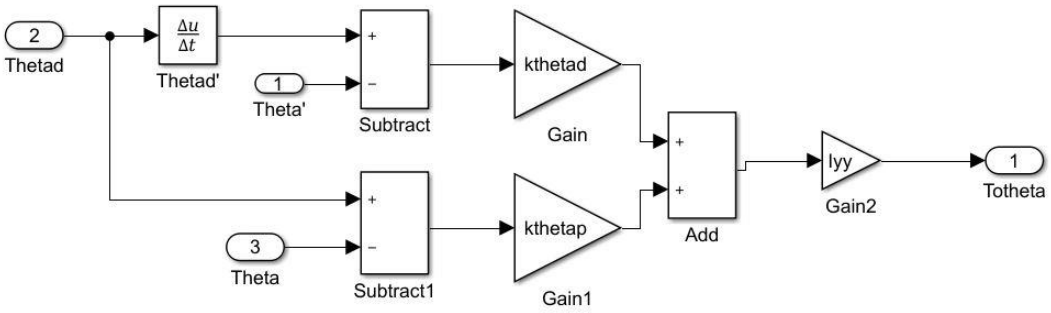

Figure B6. Pitch Control

$$\tau_{\psi} = \left(K_{\psi,D}\left(\dot{\psi}_d - \dot{\psi}\right) + K_{\psi,P}\left(\psi_d - \psi\right)\right) I_{zz},$$

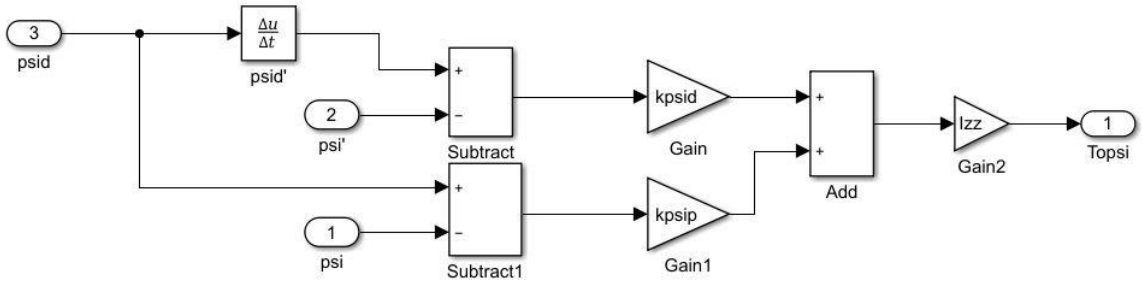

Figure B7. Yaw control

VITA

Kuldeep Singh was born in Jaipur, Rajasthan, India. He earned his Bachelor of Technology (B.Tech) degree in Mechanical Engineering from Poornima College of Engineering, Jaipur, India in 2015. He has been enrolled for his Master's degree in Texas A&M University Kingsville since Fall of 2016.